International Journal of Pharmaceutics 646 (2023) 123421

Contents lists available at ScienceDirect

International Journal of Pharmaceutics

journal homepage: www.elsevier.com/locate/ijpharm

The use of liposomes functionalized with the NFL-TBS.40–63 peptide as a targeting agent to cross the *in vitro* blood–brain barrier and target glioblastoma cells

Adélie Mellinger [a,b], Larissa J. Lubitz [c], Claire Gazaille [a], Gero Leneweit [c], Guillaume Bastiat [b], Claire Lépinoux-Chambaud [a], Joël Eyer [b,*]

[a] GlioCure SA, Angers, France
[b] Univ Angers, Inserm, CNRS, MINT, Angers, France
[c] Abnoba GmbH, 75223 Niefern-Oeschelbronn, Germany

ARTICLE INFO

Keywords:
Cell-penetrating peptides
NFL-TBS.40–63 peptide
Liposomes
Blood-brain barrier
Glioblastoma

ABSTRACT

Glioblastoma is the most common and aggressive brain tumor. Current treatments do not allow to cure the patients. This is partly due to the blood–brain barrier (BBB), which limits the delivery of drugs to the pathological site. To overcome this, we developed liposomes functionalized with a neurofilament-derived peptide, NFL-TBS.40–63 (NFL), known for its highly selective targeting of glioblastoma cells. First, *in vitro* BBB model was developed to check whether the NFL can also promote barrier crossing in addition to its active targeting capacity. Permeability experiments showed that the NFL peptide was able to cross the BBB. Moreover, when the BBB was in a pathological situation, i.e., an *in vitro* blood–brain tumor barrier (BBTB), the passage of the NFL peptide was greater while maintaining its glioblastoma targeting capacity. When the NFL peptide was associated to liposomes, it enhanced their ability to be internalized into glioblastoma cells after passage through the BBTB, compared to liposomes without NFL. The cellular uptake of liposomes was limited in the endothelial cell monolayer in comparison to the glioblastoma one. These data indicated that the NFL peptide is a promising cell-penetrating peptide tool when combined with drug delivery systems for the treatment of glioblastoma.

1. Introduction

Glioblastoma multiforme (GBM) is the most common, aggressive and malignant brain tumor in adults representing around 80 % of all primary malignant tumors of the central nervous system (Ostrom et al., 2022). Its incidence ranges from 0.59 to 5 per 100,000 persons, and it increases in many countries probably because of an aging population, overdiagnosis, ionizing radiation, air pollution and other environmental factors (Grech et al., 2020). Unfortunately, the patient prognosis is dramatic with a median survival of 12–15 months (Johnson and O'Neill, 2012; Louis et al., 2007; Van Meir et al., 2010) and a 5-years survival rate of 5.5 % (Ostrom et al., 2017; Wu et al., 2021). Despite current therapeutic strategy including surgical resection, when the tumor is accessible, radiotherapy and chemotherapy (Oike et al., 2013), GBM remains a difficult tumor to treat and presents many physiological challenges. The presence of the blood–brain barrier (BBB) is one of these major obstacles.

The BBB is a physiological barrier between blood and brain and plays a role in regulating the microenvironment (Abbott, 2002). It is formed by specific endothelial cells linked together by tight junctions (Abbott et al., 2010) restricting the permeability and delivery of potential therapies into the brain (Blakeley, 2008; Gloor et al., 2001; Groothuis, 2000; Lipinski et al., 2001; Pardridge, 2002). Therefore, new strategies to facilitate the drug passage through the BBB and the targeting of GBM cells are needed.

Currently, three major strategies exist to bypass the BBB. One of them consists in modulating the BBB by chemical or physical stimuli to improve BBB permeability (Obermeier et al., 2013). Recently, there has been a growing interest in using low-intensity focused ultrasound. This method enables to disrupt the BBB in a reversible manner. This alteration of BBB allows a therapeutic window of up to four hours

* Corresponding author.
E-mail addresses: adelie.mellinger@univ-angers.fr (A. Mellinger), lubitz@abnoba.de (L.J. Lubitz), claire.gazaille@gliocure.com (C. Gazaille), leneweit@abnoba.de (G. Leneweit), guillaume.bastiat@univ-angers.fr (G. Bastiat), claire.lepinoux-chambaud@gliocure.com (C. Lépinoux-Chambaud), joel.eyer@univ-angers.fr (J. Eyer).

https://doi.org/10.1016/j.ijpharm.2023.123421
Received 15 April 2023; Received in revised form 24 July 2023; Accepted 15 September 2023
Available online 16 September 2023

Abbreviations:

BBB	Blood-brain barrier
BBTB	Blood-brain tumor barrier
CPP	Cell penetrating peptide
DAPI	4′6-diaminido-2-phenylindole
DDS	Drug delivery system
DiD	1,1-Dioctadecyl-3,3,3,3-tetramethylindodicarbocyanine
DLS	Dynamic light scattering
DPBS	Dulbecco's Phosphate Buffered Saline
DPPC	1,2-Dipalmitoyl-*sn*-glycero-3-phosphocholine
DSPE-PEG	1,2-Distearoyl-*sn*-glycero-3-phosphoethanolamine-n-(polyethylene glycol) Ellman's Reagent 5,5′-Dithio-bis-(2-nitrobenzoic acid)
FAM	Carboxyfluorescein
GBM	Glioblastoma multiforme
kFGF	Kaposi fibroblast growth factor
LNCs	Lipid nanocapsules
mol%	Mol percent
PEG2k-Mal	Methoxy-(polyethyleneglycol)2000-Maleimide
PEG5k-Mal	Methoxy-(polyethyleneglycol)5000-Maleimide
NFL	NFL-TBS.40–63
PdI	Polydispersity index
PEG	Polyethylene glycol
TCEP	Tris-(2-carboxyethyl)-phosphine
TEER	Transendothelial electrical resistance
TJ	Tight junction
ZO-1	Zonula occludens-1

immediately after treatment (Downs et al., 2015; Sheikov et al., 2008; Wei et al., 2021). However, this delay may present risks of molecule transport that can be toxic for the brain.

Another approach to bypass the BBB is to change the administration method (intranasal or local drug delivery instead of oral and intravenous administrations) (Bruinsmann et al., 2019; Chung et al., 2020; Saka et al., 2019). However, these methods allow the administration of only a limited dose of drug and it is sometimes difficult to reach the tumor area in the brain, especially for large molecules (Tai et al., 2022).

The last strategy consists in developing a noninvasive drug delivery system (DDS), using nanocarriers (Alexander et al., 2019; Juhairiyah and de Lange, 2021; Khan et al., 2018), modified with ligands capable of targeting GBM cells without disrupting the BBB integrity (Oller-Salvia et al., 2016). Among nanoparticles, liposomes are vesicles formed by lipid bilayers surrounding an aqueous core. Natural phospholipids are most often used to mimic biological membranes, such as phosphatidylcholine, facilitating their incorporation into bilayers. Furthermore, optimization with cholesterol improves their stability and modulates the physical properties and dynamics of membranes where it is found (Briuglia et al., 2015). The addition of 1,2-Distearoyl-*sn*-glycero-3-chains phosphoethanolamine-Poly(ethylene glycol) (DSPE-PEG) makes liposomes stealthier and increases their circulation time in the blood (Mozar and Chowdhury, 2018). Moreover, to increase brain delivery efficiency, surfaces of liposomes can be modified with ligands, such as endogenous molecules, antibodies or cell-penetrating peptides (Oller-Salvia et al., 2016).

Cell-penetrating peptides (CPPs) are a group of short amphiphilic and/or cationic peptides (< 30 amino acids). It has been shown that several CPPs can be used to functionalize nanocarriers to cross cell membrane bilayers and facilitate the transport across the BBB (Van Tellingen et al., 2015). In a recent study published in 2018, Tongcheng Dai et al. have functionalized liposomes surface with CDX and iRGD peptides. Using the FRET method, authors have demonstrated the ability of liposomes to remain intact after crossing the *in vitro* and *in vivo* BBB and blood–brain tumor barrier (BBTB) (Dai et al., 2018). Another DDS was designed by Bruna Dos Santos R. et al. as dual-functionalized liposomes with a transferrin and CPP derived from the Kaposi fibroblast growth factor (kFGF). This study demonstrated that surface modification with transferrin and CPP enhanced the passage and targeting efficiency of the nanoparticles (Dos Santos Rodrigues et al., 2020b).

Among the existing CPPs, the NFL-TBS.40–63 (NFL) peptide is derived from the neurofilament low subunit-tubulin binding site 40–63. This peptide, depending on the concentrations tested, revealed targeting properties, like a CPP, and anti-tumor activity, like a cytoskeletal drug. Studies have demonstrated its ability to bind β-tubulin in glioblastoma cells, thus altering their microtubule network and reducing their proliferation and viability. Moreover, this NFL peptide demonstrated *in vitro* and *in vivo* highly selective targeting capacity of GBM cells (stem and differentiated) (Berges et al., 2012a; Lépinoux-Chambaud and Eyer, 2019). It has also been used to functionalize the surface of various nanocarriers as lipid nanocapsules (LNCs) (Balzeau et al., 2013; Karim et al., 2018; Lainé et al., 2012), magnetic porous silicon nanorods (Chaix et al., 2022) and gold nanoparticles (Arib et al., 2022). These surface modifications by the peptide showed an improvement in their targeting efficiency, in particular in human, rat or mouse GBM cells (Balzeau et al., 2013; Karim et al., 2018; Lainé et al., 2012) but also in pancreatic ductal adenocarcinoma cells (Arib et al., 2022). All these studies therefore confirmed the ability of the NFL peptide to be used as a CPP on various nanoparticles. However, no study has previously demonstrated the capacity of the NFL peptide to target GBM cells after BBB passage.

Firstly, this study focused on evaluating the ability of the peptide to cross *in vitro* BBB and BBTB. Secondly, liposomes were used as a nanoparticle model coupled with the NFL peptide to enhance the targeting of GBM cells after passage through the BBTB. To do that, *in vitro* cytotoxicity assays were performed to assess biocompatibility of liposomes alone or modified with the NFL peptide. A comparative cellular internalization into human GBM (U-87 MG) and murine endothelial (b.End3) cells was performed and confirmed by flow cytometry and confocal microscopy studies. Finally, the ability of the peptide and functionalized liposomes to cross the endothelial barrier was performed by using BBB and BBTB *in vitro* models.

2. Material and methods

2.1. Preparation of peptides and PEGylated peptides

The NFL-TBS.40–63 peptide (YSSYSAPVSSSLSVRRSYSSSSGS) coupled to 5-carboxyfluorescein (FAM-NFL; 2846 g/mol) was synthesized by Polypeptide Group (Strasbourg, France). The peptide was also synthesized and modified by adding the sequence GGGC at the Cter-minus (FAM-NFL-GGGC; 3120 g/mol) by GenScript Group (New Jersey, USA).

To conjugate FAM-NFL-GGGC to maleimide-polyethylene glycol with two different chain lengths (PEG2k as well as PEG5k), a FAM-NFL-GGGC solution (2 mg/mL) was prepared in 10 mM histidine at pH 7.4 with a 10-fold molar excess of Tris-(2-carboxyethyl)-phosphine (TCEP) (Carl Roth GmbH & Co. KG; Karlsruhe, Deutschland) for activation. To this peptide solution, a 20-fold molar excess of the PEGylation reagent, DSPE-PEG2k-Mal (Nanocs Inc; New York, USA) or DSPE-PEG5k-Mal (Biopharma PEG; Watertown, USA), was added and incubated on the rotary wheel under light protection for 24 h at room temperature. As an evidence of successful conjugation, Ellman's test (ChemCruz Biochemicals from Santa Cruz; Texas, USA) is performed, which is based on the detection of sulfhydryl groups and thus serves as evidence for free cysteines, i.e. unbound NFL. This test is performed both before conjugation with the FAM-NFL-GGGC activated by TCEP and after

conjugation with the liposomes. After conjugation, purification and final sterile filtration, only 3.2% free sulfhydryl groups are present compared to the peptide solution before conjugation.

After 24 h of incubation, the PEGylated FAM-NFL-GGGC was purified via dialysis using Slide-A-Lyzer® Cassettes (Thermo Fisher Scientific; Massachusetts, USA) with a molecular weight cutoff of 3.5 or 7 kDa depending on the PEG chain length. The dialysis medium consisted of 10 mM histidine (Carl Roth GmbH & Co. KG; Karlsruhe, Germany) buffer at pH 7.4 and was 300-fold the volume of the sample, which was exchanged after 2, 4 and 24 h.

As a final step, the samples were concentrated using the Pierce™ Protein Concentrator 3 K MW/CO (Thermo Fisher Scientific; Massachusetts, USA) with a molecular weight cutoff of 3 kDa. The devices were centrifuged at 4000 × g for 90 min in a swinging bucket rotor.

The peptides alone or PEGylated were dissolved in sterile final buffer composed of 10 mM histidine and 300 mosmol/L NaCl (Carl Roth GmbH & Co. KG; Karlsruhe, Germany) at pH 7.4 and at the concentration of 1 .

2.2. Preparation of liposomes

The liposomes were prepared by hydrating the lipid film in a buffer of 10 mM histidine and 300 mosmol/L NaCl at pH 7.4. Liposome extrusion was performed in two steps: 1) five-fold extrusion of liposomes through a track-etched polycarbonate membrane with a pore size of 400 nm and 2) 20-fold extrusion through a membrane with a pore size of 100 nm. The extrusion was carried out under argon for pressurization in the pressure range of 10 to 25 bars. DSPE-PEG2k-Mal and DSPE-PEG5k-Mal, respectively, were included at 1 mol% in the liposomes used for post-conjugation of FAM-NFL-GGGC after extrusion and optional homogenization.

After extrusion, the conjugation of the FAM-NFL-GGGC peptide to the maleimides of the PEG2k/PEG2k-Mal or PEG2K/PEG5k-Mal liposomes was carried out. For this, a precise quantity of FAM-NFL-GGGC solution (1 mg/mL) previously activated with an excess of TCEP was added. Thus, the molar ratio of the maleimide groups to the FAM-NFL-GGGC peptide was 1.2/1. The reaction took place on a rotating wheel for 24 h at room temperature. Before and after conjugation, the determination of the sulfhydryl group was carried out using Ellman's reagent.

After conjugation of the peptide to maleimide-functionalized liposomes in 10 mM histidine buffer pH 7.4, the non-conjugated NFL peptide and excipients of the conjugation reaction (e.g. TCEP) were first eliminated by dialysis using a Spectra/Por® Biotech CE tube (Carl Roth GMbH & Co. KG; Karlsruhe, Germany) with a molecular weight cutoff of 100 kDa to remove unreacted FAM-NFL-GGGC. Dialysis was also performed with 10 mM histidine buffer of pH 7.4 according to the time scheme for buffer exchange: a) 2 h, b) 4 h and c) 16 h. After dialysis, the liposomes were re-buffered by ultracentrifugation at 60 000 × g for 90 min by removing the supernatant and the resulting pellet was resuspended with 10 mM histidine and 300 mosmol/L NaCl at pH 7.4 and the suspensions were sterile filtered through a filter with syringe with a pore size of 0,22 μm PVDF-syringe filter (Carl Roth GmbH & Co. KG, Karlsruhe Germany). In a final step, they were analyzed for their cholesterol content using a cholesterol assay kit (FujiFilm Wako Chemicals Europe GmbH; Neuss, Deutschland).

2.3. Characterization of liposomes

After extrusion, the average liposomal hydrodynamic diameter distribution and polydispersity index (PdI) of liposomes were measured using dynamic light scattering (DLS). Liposomes were diluted at 1:100 in reverse osmosis water (Aquaphore®; Paris, France), and three consecutive measurements were performed. A PdI value < 0.25 indicates an unimodal hydrodynamic diameter distribution. Each sample measurement was run in triplicate at 25 °C at an angle of 173° with the Zetasizer Nano ZS (Malvern Instruments, Worcestershire, UK).

2.4. In vitro studies

2.4.1. Cell culture and reagents

U-87 MG human GBM cells and b.End3 murine endothelial cells were obtained from European Collection of Animal Cell Cultures (ECACC 89081402 and ECACC 96091929 respectively - Sigma-Aldrich; Saint-Louis, USA). They were cultured in Dulbecco′s modified Eagle′s medium high glucose (DMEM, Gibco; Dardilly, France) supplemented with 10 % of fetal bovine serum (Corning), 10 units of penicillin, 10 mg of streptomycin (Sigma-Aldrich; Saint-Louis, USA), and 1 % of non-essential amino acids (Lonza; Verviers, Belgium). Cell lines were cultured and maintained at 37 °C in a humidified atmosphere with 5 % CO_2.

2.4.2. Viability assay

Cells were seeded in 96-well plates at 1,000 and 5,000 cells per well for b.End3 murine endothelial cells and U-87 MG human GBM cells, respectively, and incubated for 24 h at 37 °C and 5 % CO_2. Then, the culture media was removed and cells were treated for 72 h at 37 °C and 5 % CO_2 with different concentrations of peptides (0.00043; 0.00215; 0.0043; 0.0215; 0.043; 0.215; 0.43; 2.15 and 4.3 μM) or liposomes (0.043; 0.215; 0.43; 2.15; 4.3; 21.5; 43; 215 and 430 μM) diluted in fresh media. Cell viability was measured using the MTS viability assay (ab197010 – Abcam; Paris, France). After rinsing the cells with 1X DPBS (Dulbecco's Phosphate Buffered Saline – Gibco; Dardilly, France), 20 μL of MTS reagent was added to each well for 2 h. The number of living cells is directly proportional to the absorbance measured by the amount of light absorbance at 490 nm in a SpectraMax M2 multi-scanning spectrophotometer (Molecular Devices, San Jose, California, USA).

2.4.3. Flow cytometry

Cells were seeded in 6-well plates at 400,000 cells per well and were incubated for 24 h at 37 °C and 5 % CO_2. Then, the culture media was removed and cells were treated at 37 °C and 5 % CO_2 with different concentrations of peptides (1; 5; 10 and 25 μM) for 6 h or liposomes (5; 10; 25; 50 and 100 μM) for 1 or 6 h diluted in fresh media. After incubation, cells were washed with 1X DPBS and with free DMEM, and the cells were incubated with 1X Trypsin (Gibco; Dardilly, France) for 5 min. Cells were centrifuged at 250 G for 5 min, washed twice with 1X DPBS and counterstained with Propidium Iodide (50 μg/mL, P4867 - Sigma-Aldrich; Saint-Louis, USA) before analysis on a BD FACSCantoTM II System (BD Biosciences; Paris, France) and using the FlowJo Software (BD Biosciences; Paris, France). 10,000 cells were measured for each condition.

To understand the molecular mechanism of cell penetration, U-87 MG human GBM cells and b.End3 murine endothelial cells were seeded in 6-well plates at 400,000 cells per well for 24 h. The cells were then incubated at 37 °C or at 4 °C for 1 h and then treated with 25 or 100 μM liposome formulations for 1 h. The cells were washed with 1X DPBS and incubated for 5–10 min with 1X Trypsin to detach the cells. After centrifugation, cells were re-suspended in 50 μg/mL Propidium Iodide and analyzed by flow cytometry. 10,000 cells were measured for each condition.

2.4.4. Immunocytochemistry

To visualize the treatment internalization, 20,000 and 35,000 cells per well for b.End3 murine endothelial cells and U-87 MG human GBM cells, respectively, were seeded in 24-well plates containing one coverslip previously coated with poly(d)lysine (0.1 mg/mL per well and washed three times with 1X DPBS - Sigma-Aldrich; Saint-Louis, USA) and incubated for 24 h at 37 °C and 5 % CO2. Then, the cells were treated with FAM-NFL and FAM-NFL-GGGC peptides (50 μM) or with liposome formulations for 6 h at 37 °C. At the end of the incubation time, cells were washed three times with 1X DPBS and fixed with 4 % paraformaldehyde (15714; Delta microscopies; Mauressac, France) for 10 min at room temperature. Then, cells treated with peptides were permeabilized with 0.2 % triton X-100 (T9284 - Sigma-Aldrich; Saint-Louis,

USA) for 10 min, and blocked with 5 % bovine serum albumin (A7030 - Sigma-Aldrich; Saint-Louis, USA) for 30 min at room temperature. Cells were incubated with a mouse anti-α tubulin antibody at 1:250 (ab7750 - Abcam; Paris, France) overnight at 4 °C. The primary antibody was revealed with anti-mouse Alexa Fluor 568 at 1:500 (A11004 - Thermo Fisher Scientific; Massachusetts, USA) for 1 h at room temperature. Then, cells were incubated with 4′6-diaminido-2-phenylindole at 1 μM (DAPI, D9542 - Sigma-Aldrich; Paris, France) for 10 min at room temperature. For cells treated with liposomes, only nuclei were labelled with 1 μM of DAPI for 10 min at room temperature. All coverslips were mounted with the Prolong Gold Antifade reagent (P36930 - Thermo Fisher Scientific; Massachusetts, USA). Cells were observed with a confocal microscope (Leica TCS SP8; Leica Biosystems, Nanterre, France).

2.4.5. Establishment and characterization of in vitro BBB and BBTB models

The *in vitro* endothelial barrier was constructed by the combination of b.End3 murin endothelial cells on the luminal side (upper compartment) and U-87 MG human GBM cells on the abluminal side (lower compartment) of the culture insert. Each cell line was seeded overnight at 37 °C and 5 % CO_2 in 6 or 24-well plates with 50,000 b.End3 cells per cm^2 on polyester Transwell inserts (0.4 μm pore size; Sarstedt Marnayn, France) coated with collagen I to mimic the *in vitro* BBB, or with 50,000 U-87 MG cells per cm^2 in separate plates (without insert) to allow cell adhesion. The following day, the two cell lines were cocultured to mimic the *in vitro* BBTB by placing the b.End3 inserts in 6 or 24-well plates containing the U-87 MG cells. The *in vitro* BBB and BBTB models were maintained in culture for 7 days to form a tight barrier (Fig. 1A-B). The medium was replaced every 2–3 days and cells were checked for confluence by optical microscopy observations.

The integrity of the barrier was determined by measuring trans-endothelial electrical resistance (TEER) using EVOM2 (World Precision Instruments; USA). The TEER of endothelial barriers was also recorded throughout the experiment to monitor any possible cytotoxicity and loss of integrity after liposomes treatment.

To characterize the tight junctions of the endothelial barriers, b.End3 murine endothelial cells (cultured on inserts) were fixed after 7 days of incubation with 4 % paraformaldehyde. Cells were incubated with primary anti-ZO-1 antibody diluted in 0.1 % of Saponine (Acros; Geel, Belgium) and 5 % bovine serum albumin at 1:250 (Thermo Fisher Scientific; Massachusetts, USA) overnight at 4 °C. The primary antibody was revealed with anti-mouse Alexa Fluor 568 at 1:500 (A11004 - Thermo Fisher Scientific; Massachusetts, USA) for 1 h at room temperature and nuclei were labelled with 1 μM of DAPI for 10 min at room temperature before the mounting with coverslips.

The permeability of each *in vitro* model was checked by measuring the flux of fluorescein isothiocyanate (FITC) conjugated to Dextrans of different molecular weight (FITC-Dextran 4, 40 and 70 kDa) across the endothelial barriers. Briefly, after 7 days of culture, the medium in the upper compartment was replaced by medium containing 100 μg/mL of FITC-Dextran. After 6 h, the paracellular transport was evaluated by measuring the fluorescence intensity of FITC-Dextran in the lower compartment using spectrophotometer microplate reader at excitation/emission wavelengths of 485/535 nm respectively (SpectraMax® M2). Then, the percentage of FITC-Dextran transport was calculated by measuring the quantity of FITC-Dextran across endothelial barrier of both models.

2.4.6. In vitro transport across the BBB and BBTB models and glioblastoma targeting ability of NFL-peptide alone or coupled with liposomes

Cells were seeded and cultured as described in 2.4.5. to obtain BBB and BBTB models. After 7 days of culture, the culture medium in upper compartment was replaced with medium containing 30 μM of each peptide or 100 μM of different DiD-liposomal formulations. After 6 and 24 h of treatment, the fluorescent intensity was measured in the lower chambers and the percentage of compound transported across the endothelial barrier was evaluated.

To visualize if compounds were internalized in U-87 MG human GBM cells, once the endothelial cell barrier crossed, the same procedure of section 2.4.3 were applicated.

2.4.7. Statistical analysis

Data were presented as means ± SEM. Statistical differences were determined using unpaired Mann-Whitney test when comparing between two independent groups, and Kruskall-Wallis test followed by a Dunn's post-hoc test when comparing across three or more independent groups. p value < 0.05 was considered significant.

3. Results

3.1. Establishment and characterization of the in vitro BBB and BBTB models

To assess the targeting ability of NFL peptides and liposomes, BBB and BBTB *in vitro* models were developed by using murine b.End3 endothelial cells and human U-87 MG GBM cells (described in Fig. 1A-B).

After 7 days of mono- and coculture, the permeability properties of endothelial barriers were analyzed in the BBB and BBTB *in vitro* models. The TEER values were 21.80 ± 3.90 Ω.cm^2 and 13.88 ± 3.51 Ω.cm^2 for *in vitro* BBB and BBTB models respectively (Fig. 1C). For BBTB model, TEER value decreases significantly by 38 ± 3 % compared to the BBB model. Observations with optical microscopy showed that after 7 days of coculture b.End3 cells are confluent in the BBB model, whereas in the BBTB model the endothelial cell monolayer appears less dense with a decrease in cell confluence and cell–cell contacts (Fig. 1D). This phenomenon is also observed by confocal imaging in Fig. 1E. The BBB model showed a high expression of the tight junction (TJ) proteins zonula occludens-1 (ZO-1) representing the endothelial cell–cell contact. In the BBTB model, the ZO-1 protein expression is reduced compared to the endothelial barrier of BBB model (Fig. 1E). The passage of FITC-Dextrans (4, 40 and 70 kDa) from luminal compartment to abluminal compartment was measured and expressed as relative percentage of crossing FITC-Dextran (Fig. 1F). The relative percentage of crossing is higher for FITC-Dextran 4 kDa (16.18 ± 2.03 % for BBB and 20.24 ± 1.41 % for BBTB) than for FITC-Dextrans 40 kDa and 70 kDa with percentages around 4.46 % for BBB model and 5.96 % for BBTB model.

3.2. Cellular viability and internalization in b.End3 endothelial and U-87 MG GBM cells after treatment with the peptides

To couple the FAM-tagged NFL-TBS.40–63 peptide with the DSPE-PEG-Maleimide chains (Mw of the PEG moiety: 2000 or 5000 Da), the peptide was modified by adding a GGGC linker sequence (Table 2). The conjugation of FAM-NFL-GGGC peptide was performed between the sulphur group of the cysteine and the Maleimide end group of the PEG chains at the DSPE and formed a stable bond. To verify whether the GGGC binding sequence and the PEG chains do not render the peptide toxic at the concentrations tested and do not alter the targeting of GBM cells, cytotoxicity and internalization analyzes were carried out on b.End3 and U-87 MG in the presence of the modified peptides.

After 72 h of exposure with increasing concentrations of the different peptides, the cell viability was>85 % up to 4.3 μM for both cell lines. In addition, no modification of morphology and confluence of cells were observed after treatment with the highest concentration of peptides (4.3 μM) compared to untreated cells (Medium alone). These results showed that at the concentrations tested, the peptides are not toxic to cells (Fig. 2A).

To investigate the capacity of the peptide to enter murine b.End3 endothelial and human U-87 MG GBM cells, they were incubated with increasing concentrations of the various FAM-NFL peptides coupled or not with DSPE-PEG-Maleimide chains (PEG2k or PEG5k) following 6 h

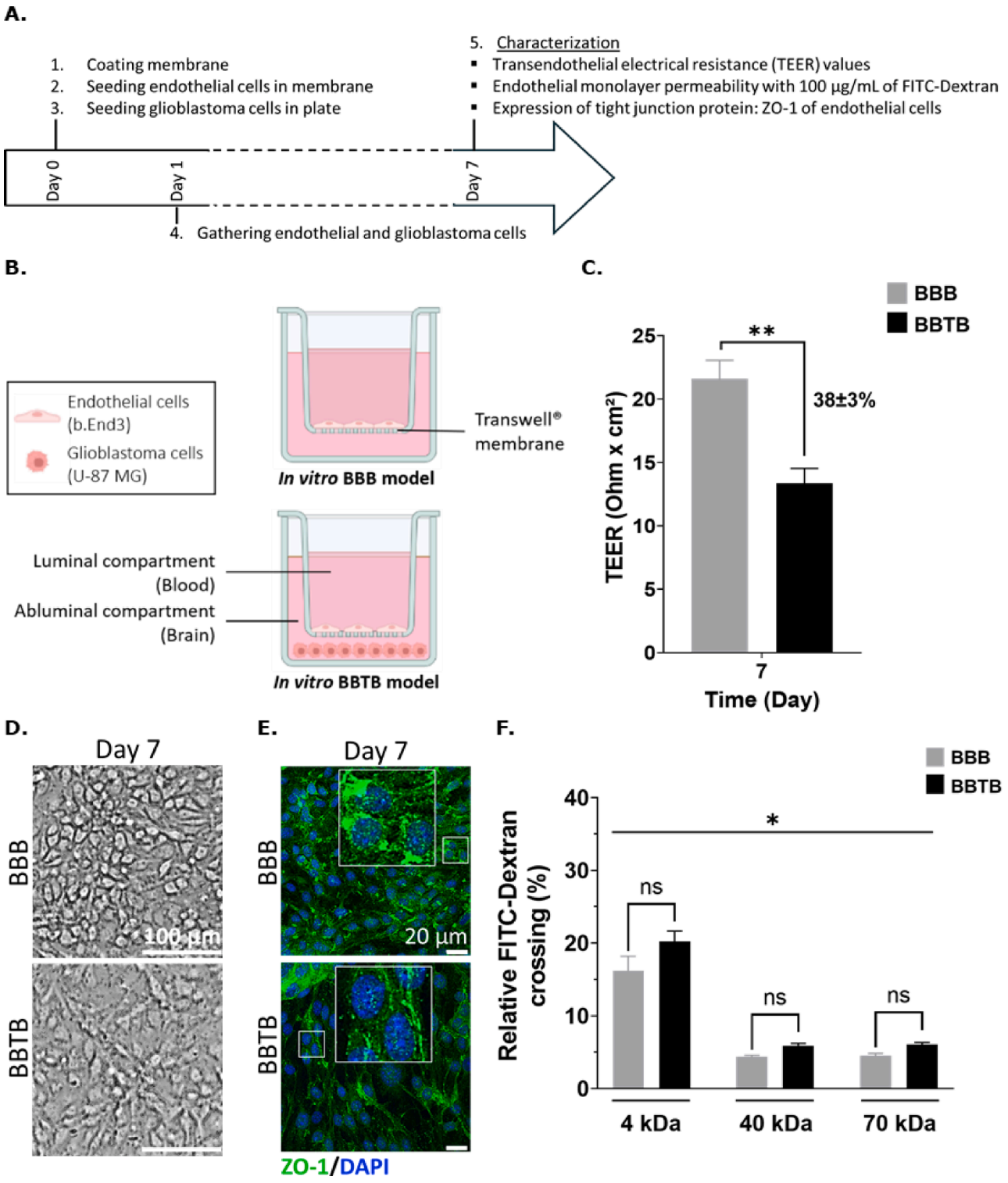

Fig. 1. Characterization of the *in vitro* BBB and BBTB models. A) Timeline and procedure of the *in vitro* BBB and BBTB models establishment and characterization. B) Schematic illustration of the *in vitro* BBB and BBTB models. C) The permeability of both models was assessed by TEER measurement (Ohm × cm^2) of *in vitro* BBB (grey) and BBTB (black) models at 37 °C and was expressed as mean ± SEM after subtraction of the mean value obtained with inserts without cells. Experiments were performed at least 8 times (n = 8). Statistical analysis: Mann-Whitney test (**$p < 0.01$). D) Images illustrating the confluence and integrity of endothelial monolayer cells (b.End3) after 7 days of culture in coculture or not with GBM cells (U-87 MG) at 37 °C. Images were taken with a confocal microscope. Scale bars: 100 µm. E) An immunocytochemistry of the endothelial monolayer cells of *in vitro* BBB and BBTB models was realized to reveal tight junctions (anti-ZO-1, green) and nuclei (DAPI, blue). Experiments were performed at least 3 times (n = 3). Scale bars: 20 µm. F) The endothelial monolayer cells of *in vitro* BBB (grey) and BBTB (black) models were treated for 6 h at 37 °C with 100 µg/mL of FITC-dextran at different molecular weights (4, 40 and 70 kDa). The permeability of both models was assessed by calculating the quantity of FITC-dextran in abluminal compartment compared to the initial quantity in luminal compartment and was expressed as relative FITC-dextran crossing percentage (at the equilibrium between each compartment). Experiments were performed at least 3 times (n = 3–5). Data are represented as mean ± SEM. Statistical analysis: Kruskall-Wallis test and a Dunn's post-hoc test (ns $p > 0.05$ and *$p < 0.05$). (For interpretation of the references to colour in this figure legend, the reader is referred to the web version of this article.)

Table 2
Composition of liposomal formulations.

Liposomes	Composition (molar ratio, %)
Control	DPPC/Chol/DiD (59.5/40/0.5)
PEG2k	DPPC/Chol/DSPE-PEG2k/DiD (54.5/40/5/0.5)
PEG2k/ PEG2k-Mal	DPPC/Chol/DSPE-PEG2k/DSPE-PEG2k-Mal/DiD (53.5/40/5/1/0.5)
PEG2k/ PEG5k-Mal	DPPC/Chol/DSPE-PEG2k/DSPE-PEG5k-Mal/DiD (53.5/40/5/1/0.5)
PEG2k/PEG2k-Mal-FAM-NFL	DPPC/Chol/DSPE-PEG2k/DSPE-PEG2k-Mal-FAM-NFL-GGGC/DiD (53.5/40/5/1/0.5)
PEG2k/PEG5k-Mal-FAM-NFL	DPPC/Chol/DSPE-PEG2k/DSPE-PEG5k-Mal-FAM-NFL-GGGC/DiD (53.5/40/5/1/0.5)

of incubation. Flow cytometry analysis showed a dose-dependent internalization of all peptides to both cell lines, especially well demonstrated regarding the median fluorescence intensity (Fig. 2B). Moreover, FAM-NFL-GGGC-Mal-PEG2k or FAM-NFL-GGGC-Mal-PEG5k displayed higher uptake than FAM-NFL modified or not with GGGC sequence. As shown in Fig. 2B, at 1 μM both FAM-NFL coupled with DSPE-PEG-Maleimide chains showed >35 % of cellular uptake in b.End3 and U-87 MG. However, even if the peptides enter both cell lines, their internalization was more important in U-87 MG cells than in b.End3 cells, demonstrating by a higher median fluorescence intensity, especially for FAM-NFL-GGGC coupled with DSPE-PEG5k-Mal ($p < 0.05$). For example, the median fluorescence intensity was 2.5 and 4.6 times elevated in U-87 MG cells when treated with 25 μM of FAM-NFL-GGGC-Mal-PEG2k and FAM-NFL-GGGC-Mal-PEG5k peptides, respectively.

The fluorescence images in Fig. 2C show the uptake of FAM-NFL-GGGC and FAM-NFL-GGGC-Mal-PEG5k peptides in the two cell lines. The internalization seemed higher in GBM than in endothelial cells. When U-87 MG cells were treated with the FAM-NFL-GGGC-Mal-PEG5k, a strong fluorescence pattern was observed all through cytoplasm and nuclei in comparison to the other peptides.

3.3. Passage of NFL peptide through endothelial cells and internalization in U-87 MG GBM cells

To visualize the capacity of FAM-NFL peptides to cross the endothelial barriers, 30 μM of each peptide were added to the luminal (upper) chamber (Fig. 3). After 6 h of incubation, the quantity of various FAM-NFL peptides was measured in the medium from the abluminal (lower) chamber and the percentage of relative crossing peptide was calculated. A significant difference was observed, for each sample, between BBB *in vitro* model and the control insert + U-87 MG. Peptides showed a higher percentage of passage across the BBB, BBTB and insert + U-87 MG models (> 8, 10 and 13 % for BBB, BBTB and insert + U-87 MG models, respectively) compared to 4 kDa FITC-Dextran (3.62 ± 0.19, 4.51 ± 0.28 and 6.84 ± 0.57 % for BBB, BBTB and insert + U-87 MG models, respectively). This difference is significant for FAM-NFL and FAM-NFL-GGGC peptides compared to FITC-Dextran 4 kDa in the BBTB model.

After their passage through the *in vitro* BBTB model, the percentage of U-87 MG cells incorporating peptides was determined by flow cytometry. The percentage of fluorescent U-87 MG cells was higher when cells were treated with the peptides than with FITC-Dextran. Indeed, there are about 5 times more U-87 MG cells labeled with peptides than with FITC-Dextran 4 kDa for BBTB *in vitro* model and insert + U-87 MG model.

3.4. Formulation and characterization of liposomes

After showing that the FAM-NFL peptide modified with a linker and/or PEG chains retains its ability to target GBM cells and is able to cross the endothelial cell barrier, the coupling of FAM-NFL-GGGC peptide was performed on the terminal end of the DSPE-PEG (2000 or 5000)-Maleimide chain after liposome preparation. As described in Table 3, the mean particle hydrodynamic diameter of all liposomal formulations was < 150 nm excepted for PEG2k/PEG2k-Mal-FAM-NFL liposomes (222.5 nm). The polydispersity index (PdI) was lower than 0.25 for non-PEGylated and PEGylated liposomes and this value increased when the surface of liposomes was modified by FAM-NFL-GGGC peptide: 0.409 and 0.332 for PEG2k/PEG2k-Mal-FAM-NFL liposomes and PEG2k/PEG5k-mal-FAM-NFL liposomes, respectively.

3.5. Cellular viability and internalization in b.End3 endothelial and U-87 MG GBM cells after treatment with the liposomal formulations

The effect of the liposome formulations was evaluated on the viability of b.End3 and U-87 MG cells. After 72 h of exposure with increasing concentrations of different liposomes, the cell viability was>85 % up to a phospholipid concentration of 430 μM for both cell lines. In addition, for each condition, no modification of morphology and confluence of cells was observed after treatment with the higher concentration of liposomes (430 μM) compared to the untreated cells (Medium). These results showed no toxicity on either cell lines, regardless of the formulation (Fig. 4A).

To investigate the capacity of the liposomes to be internalized in b.End3 and U-87 MG cells, cells were incubated for 1 h (Supplementary Fig. 1B) or 6 h (Fig. 4B) with increasing concentrations of the liposomes. After 1 h, flow cytometry analysis showed a time and dose-dependent internalization. The presence of the PEG chains did not change the internalization of the liposomes compared to the control liposomes. On the other hand, an increase in the internalization of liposomes in the two cell lines was observed when liposomes are coupled to the peptide (Supplementary Fig. 1).

After 6 h of incubation, almost all cells have internalized the liposomes and shown a time-dependent internalization with > 90 % of fluorescent cells, except for the liposomes PEG2k and PEG2k/PEG5k-Mal with 40 to 80 % uptake into cells. Interestingly, the presence of the FAM-NFL-GGGC peptide on PEG2k/PEG2k-Mal-FAM-NFL liposomes improved significantly the amount of liposomes internalized into endothelial and GBM cells, with a preferential incorporation into GBM cells, as demonstrated with the median fluorescence intensity. On the contrary, this increase in the amount of material incorporated in the cells was not observed with liposomes PEG2k/PEG5k-Mal-FAM-NFL whose median fluorescence intensities were similar to liposomes without peptide (Fig. 4B).

The active or passive uptake mechanism of the liposomes was evaluated by incubating each cell line (b.End3 and U-87 MG cells) at 4 °C or 37 °C with 100 μM (Fig. 5A-B) of liposomes. Flow cytometry analysis showed a significant ($p < 0.05$) reduction of liposome internalization at 4 °C in both cell lines, demonstrated by a decrease in the percentage of fluorescent cells and median fluorescence intensity. These results suggest that when coupled to the FAM-NFL-GGGC, liposomes could enter U-87 MG cells both via active and passive mechanisms while they could only enter in b.End3 cells via an energy-dependent mechanism. However, when U-87 MG cells were treated with PEG2k/PEG2k-Mal-FAM-NFL for 1 h at 4 °C, the percentage of fluorescent cells and the associated median fluorescence intensity were still important compared to other conditions, even if the number of samples is not sufficient to obtain a significant difference. These results suggest that when coupled to the FAM-NFL-GGGC, liposomes could enter U-87 MG cells both via active and passive mechanisms while they could only enter in b.End3 cells via an energy-dependent mechanism.

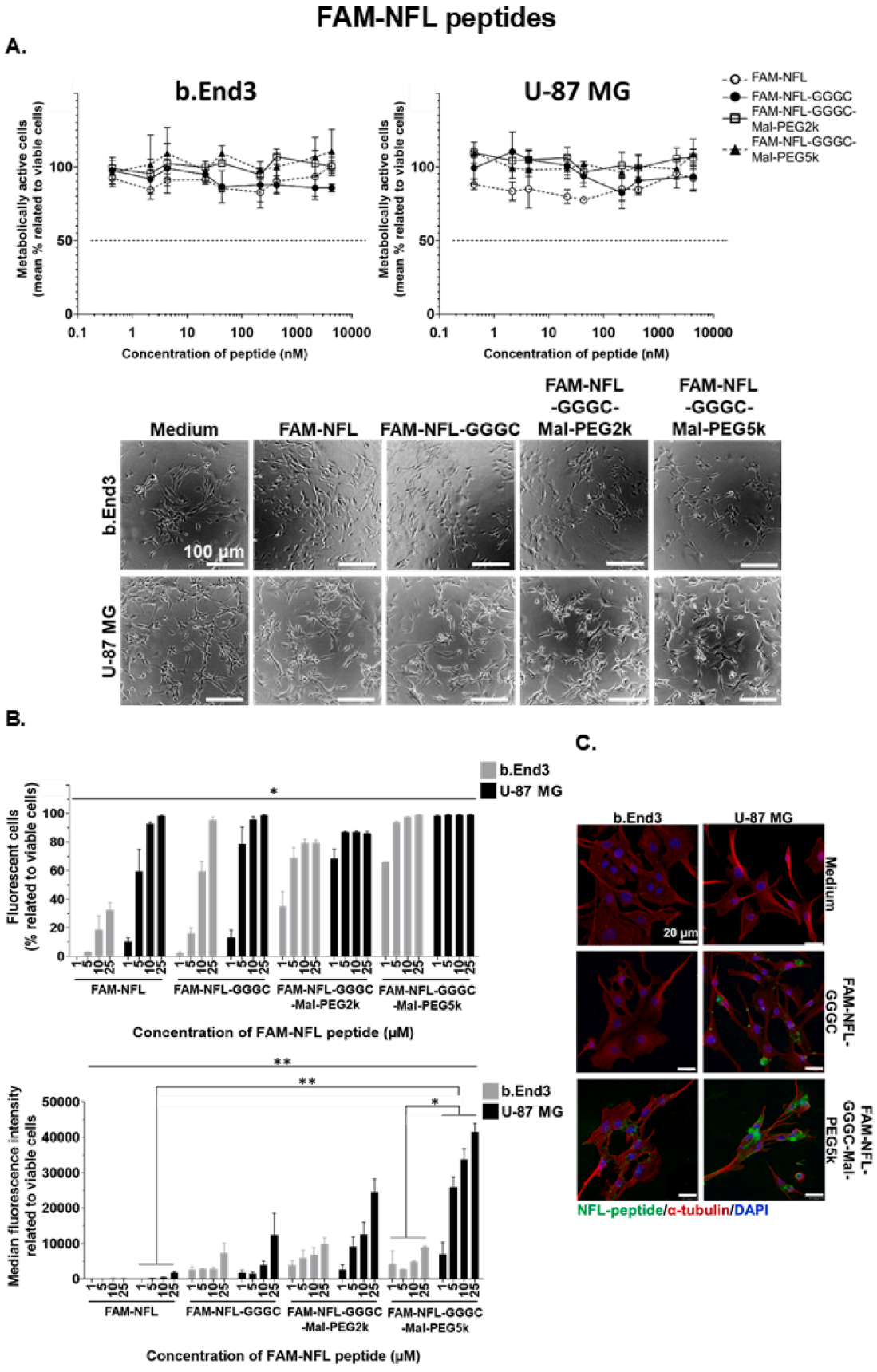

(caption on next page)

Fig. 2. *In vitro* effects of the peptides on cell viability and internalization in murine b.End3 endothelial cells and human U-87 MG GBM cells. A) Murine endothelial cells (b.End3) and human GBM cells (U-87 MG) were treated for 72 h at 37 °C with increased concentration of peptides (from 0.43 nM to 4,30 nM) and cell viability (metabolically active cells) was evaluated by MTS assay. Experiments were performed at least 3 times (n = 3) in triplicate. Data are represented as mean ± SEM. Images illustrate the morphology of cells treated with these peptides. Images were taken with an optic microscope. Scale bars: 100 μm. B) A flow cytometry analysis of murine endothelial cells (b.End3, grey) and human GBM cells (U-87 MG, black) treated with increasing concentrations of peptides (1, 5, 10 and 25 μM) for 6 h at 37 °C. Results were expressed in percentage of fluorescent cells (upper) and in median fluorescence intensity (bottom) related to viable cells. Experiments were performed at least 3 times (n = 3–5), and 10,000 cells were measured for each experiment. Data are represented as mean ± SEM. Statistical analysis: Kruskall-Wallis test and followed by a Dunn's post-hoc test (*p < 0.05 and **p < 0.01). C) b.End3 and U-87 MG cells were incubated 6 h at 37 °C without (Medium) or with 50 μM of FAM-NFL-GGGC and FAM-NFL-GGGC-Mal-PEG5k peptides. Immunocytochemistry was realized to reveal microtubules (anti-α-tubulin, red), peptide (FAM-NFL peptide, green) and nuclei (DAPI, blue). Experiments were performed at least 3 times (n = 3), and images were taken with a confocal microscope. Scale bars: 20 μm. (For interpretation of the references to colour in this figure legend, the reader is referred to the web version of this article.)

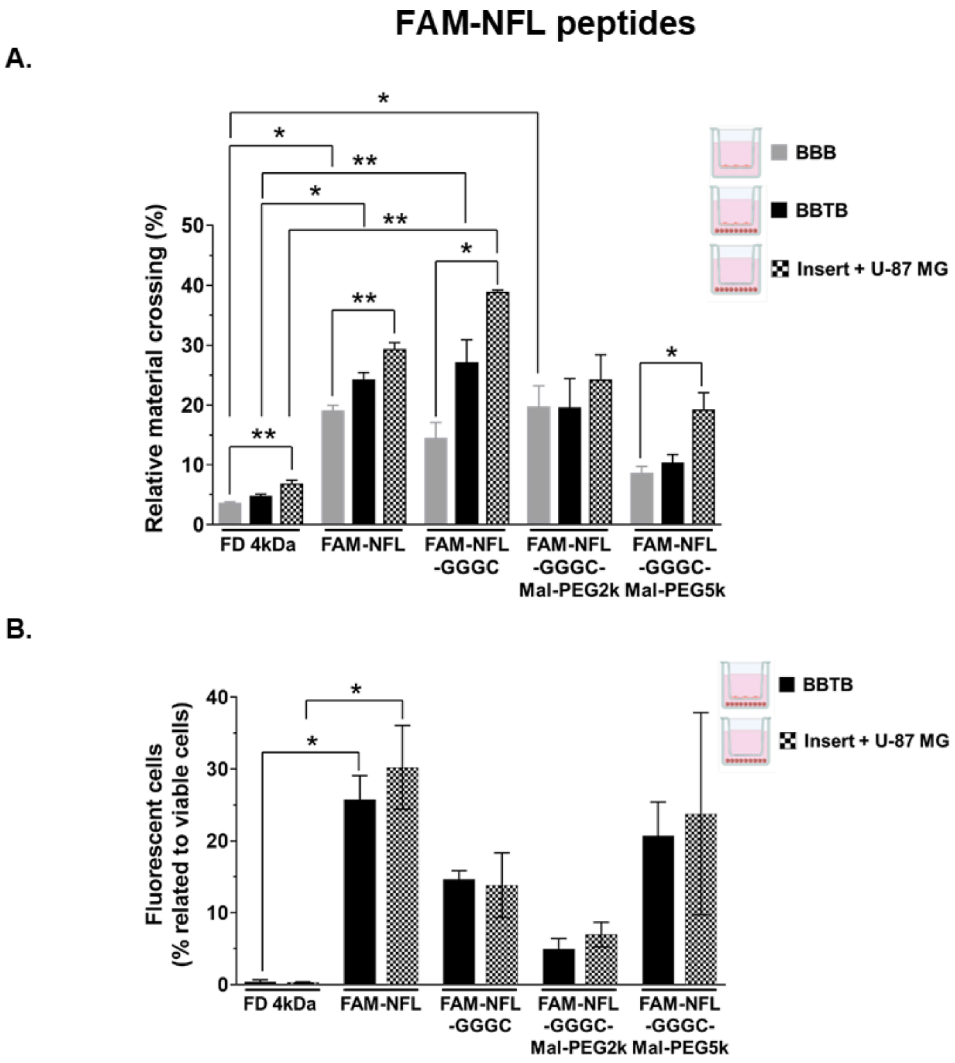

Fig. 3. Crossing of the peptides through the endothelial barrier (b.End3 cells) and their internalization in human GBM cells (U-87 MG). A) 30 μM of FITC-Dextran (4 kDa), FAM-NFL, FAM-NFL-GGGC, FAM-NFL-GGGC-Mal-PEG2k or FAM-NFL-GGGC-Mal-PEG5k peptides were added on the luminal compartment of *in vitro* BBB (grey), BBTB (black) and insert + U-87 MG (square black and white) models for 6 h at 37 °C. The permeability of each model was assessed by calculating the quantity of compound in abluminal compartment compared to the initial quantity in luminal compartment and was expressed as relative crossing material percentage (at the equilibrium between each compartment). Experiments were performed at least 3 times (n = 3–4). Data are represented as mean ± SEM. Statistical analysis: Kruskall-Wallis test and a Dunn's post-hoc test (ns p > 0.05, *p < 0.05 and **p < 0.01). B) A flow cytometry analysis of human GBM cells (U-87 MG) was realized after passage of various peptides (30 μM) through the endothelial monolayer cells for 6 h at 37 °C. Results were expressed in percentage of fluorescent cells related to viable cells. Experiments were performed at least 3 times (n = 3), and 10,000 cells were measured for each experiment. Data are represented as mean ± SEM. Statistical analysis: Kruskall-Wallis test and a Dunn's post-hoc test (*p < 0.05).

3.6. Passage of liposomes through endothelial cells and internalization in U-87 MG GBM cells

The passage of the different liposomes through *in vitro* BBB and BBTB models was then evaluated. First, the integrity of both barriers was studied after 24 h of treatment with 100 μM of different liposomes. TEER, which measures the endothelial barrier integrity, was not different between the treated and untreated conditions, meaning that liposomes do not affect it (Fig. 6A). Images of cells from BBB and BBTB models after treatment with liposomes confirmed these results.

Table 3
Composition, particle size distribution and polydispersity index of various liposomal formulations (n = 1–3). Data are represented as mean ± SD.

Liposomes	Compound				Z-average (nm)	PdI
	DSPE-PEG2k	DSPE-PEG2k-Mal	DSPE-PEG2k-Mal	FAM-NFL-GGGC		
Control	–	–	–	–	101.8 ± 3.2	0.176 ± 0.024
PEG2k	+	–	–	–	92.2 ± 14.0	0.240 ± 0.086
PEG2k/ PEG2k-Mal	+	+	–	–	84.6 ± 3.3	0.247 ± 0.031
PEG2k/ PEG5k-Mal	+	–	+	–	128.9 ± 2.7	0.115 ± 0.019
PEG2k/ PEG2k-Mal-FAM-NFL	+	+	–	+	222.5	0.409
PEG2k/ PEG5k-Mal-FAM-NFL	+	–	+	+	141.5	0.332

To evaluate the capacity of liposomes to cross the endothelial barrier, 100 μM of each liposome formulation were added to the luminal (upper) chamber for 6 (Supplementary Fig. 2A) or 24 h (Fig. 6B). Liposomes coupled with FAM-NFL-GGGC peptide showed a non-significant difference of transport as compared to control or PEGylated liposomes. After 6 and 24 h of incubation, the percentage of relative liposomes crossing endothelial cell monolayer from the BBB and BBTB models, and the insert was < 5 %. After 6 h of treatment, the percentage of U-87 MG cells incorporating liposomes was < 5 %, regardless the type of liposomes (Supplementary Fig. 2B). However, after 24 h of treatment, 16.8 ± 3.1 % of U-87 MG cells incorporated PEG2k/PEG2k-Mal-FAM-NFL liposomes (Fig. 6C), suggesting a time-dependent incorporation and demonstrating that this liposome formulation is more effective in targeting GBM cells.

4. Discussion

Delivery systems can be conjugated with CPPs on their surface to improve their specific cellular targeting (Zylberberg et al., 2017). The CPP used in this study is the NFL peptide. Injected in brain of rat bearing GBM, this peptide is still found in tumor cells 30 days after injection (Berges et al., 2012a). Moreover, 16 days after peptide injection, it is eliminated from the injection site in normal brains, and possibly from normal brain regions in tumor-bearing rats. In the past decade, literature has shown that peptides derived from NFL peptides (including biotinylated-NFL and FAM-NFL) can adsorb onto nanoparticles such as LNCs (Balzeau et al., 2013; Carradori et al., 2016; Karim et al., 2018, Griveau et al., 2022). Balzeau and Carradori works showed 45.9 and 48.3 % of biotinylated-NFL adsorption on LNCs respectively (Balzeau et al., 2013). Moreover, Karim and colleagues showed similar results with FAM-NFL onto LNCs (Karim et al., 2018). Griveau and colleagues showed that a mixture of 200 μmol/L of peptide with 30 mg/mL of LNCs gave an adsorption percentage of 95.06 ± 1.19 % and 86.23 ± 1.32 % respectively for LNC-biotinylated-NFL and LNC-FAM-NFL. The difference of adsorption between the studies could be due to the method of quantification used. Concerning the LNC-nude-NFL, the maximum adsorption obtained was 30.61 ± 11.45 %, suggesting an important role of the probe in the NFL binding capacity (Griveau et al., 2022).

To functionalize nanocarriers with CPPs, linkers are commonly used to combine PEG to other molecules. In our study, we used a GGGC linker to attach the NFL peptide to PEG chains. Bergès et *al.* showed that the internalization of the NFL peptide appears to correlate with a particular structural pattern, affected by a change in its amino acid sequence and its phosphorylation status (Berges et al., 2012b). Therefore, we investigated if the addition of the GGGC linker at the Cterm domain of NFL peptide sequence could have an impact on its capacity to target GBM cells. Altai et *al.* modified an anti-HER2 with different peptide chelators, containing a cysteine, allowing the binding of the antibody to Rhenium-188 (Altai et al., 2014). In this study, as for the NFL peptide, the authors showed that the GGGC chelator increased *in vivo* biodistribution without altering the functions of the molecules. We did not observe a reduction in the NFL peptide internalization in GBM cells and no particular toxicity, suggesting that the GGGC linker has no or a non-significant impact on the NFL peptide conformation.

In our work, we have demonstrated the increase in the hydrodynamic diameter and PdI of liposomes when the NFL peptide is coupled to PEG chains and suggest the presence of several liposome populations. Recent studies have demonstrated the ability of the biotinylated-NFL peptide to self-assemble and form nanofilaments when it reaches a critical aggregation concentration, along which LNCs can adsorb and form typical nano-bracelets (Alnemeh-Al Ali et al., 2022; Griveau et al., 2022). Based on previous work, we can explain the increase in the hydrodynamic diameter and PdI by the formation of liposome networks induced by the presence of the peptide. This could have consequence on the passage and internalization of liposomes combined to NFL peptides as Griveau and colleagues showed a lower internalization of LNC-biotinylated-NFL compared to LNC-FAM-NFL where no network was formed (Griveau et al., 2022). To confirm this hypothesis, it is necessary to vary the concentration of peptide coupled to the liposomes but also observe the liposomes by transmission electron cryomicroscopy.

Before applying liposomes and NFL on BBB and BBTB *in vitro* models, cytotoxic assays were performed on b.End3 and U-87 MG monocultures to determine the concentration of treatment to be used. The NFL peptides were well tolerated by b.End3 and U-87 MG cells at the tested concentrations (from 0.00043 to 4.3 μM). This is confirmed by Berges et al. who showed that the IC50 of the NFL peptide on U-87 MG is about 20 μM (Berges et al., 2012a). Moreover, liposomes were not toxic on b.End3 and U-87 MG cells from 0.043 to 430 μM. Constantinescu et al. showed that PEGylated cationic liposomes did not have a high impact on b.End3 cell viability after 24 h of treatment (Constantinescu et al., 2019). Moreover, other studies showed that liposomes were not toxic on U-87 MG cells (Corrêa et al., 2019; Jhaveri et al., 2018; Katona et al., 2022; Tong et al., 2015). Furthermore, Balzeau et al. observed that LNCs coupled to the NFL peptide did not show toxicity on GL261 and mouse primary astrocytes after 72 h of treatment, suggesting that the addition of the NFL peptide does not increase the toxicity of nanoparticles (Balzeau et al., 2013).

The BBB mainly consists of endothelial cells and aims to regulate the ingress of substances into the brain from the circulation (Abbott et al., 2010). We developed a BBB model with murine endothelial cells b.End3 and observed characteristics similar to those in the literature. Indeed, Booth and colleagues had a TEER value of 17 Ω.cm^2 after 5 days of culture and a high expression of ZO-1 (Booth and Kim, 2012) . TEER values are dependent on several factors. Endothelial cells of human, bovine or porcine origin have superior human BBB properties to those from rats or mice. For example, Sun and colleagues showed that the TEER measurements across the immortalized human brain microvascular endothelial cells monolayer were at least 42-fold higher than those across the b.End3 monolayer (Sun et al., 2022). Moreover, Nakagawa and colleagues showed that the TEER values of rat brain capillary endothelial cells monolayer were about 75 Ω.cm^2 (Nakagawa et al., 2009). The TEER values that we reported in our study (about 22 Ω.cm^2) are low but consistent with those listed in the literature when endothelial cells of murine origin are used (Omidi et al., 2003; Booth and Kim, 2012; Sun et al., 2022; Park et al., 2023). Indeed, Park and colleagues showed that after 7 days, the TEER value across the b.End3 monolayer was about 30 Ω.cm^2 (Park et al., 2023). Moreover, Sun and

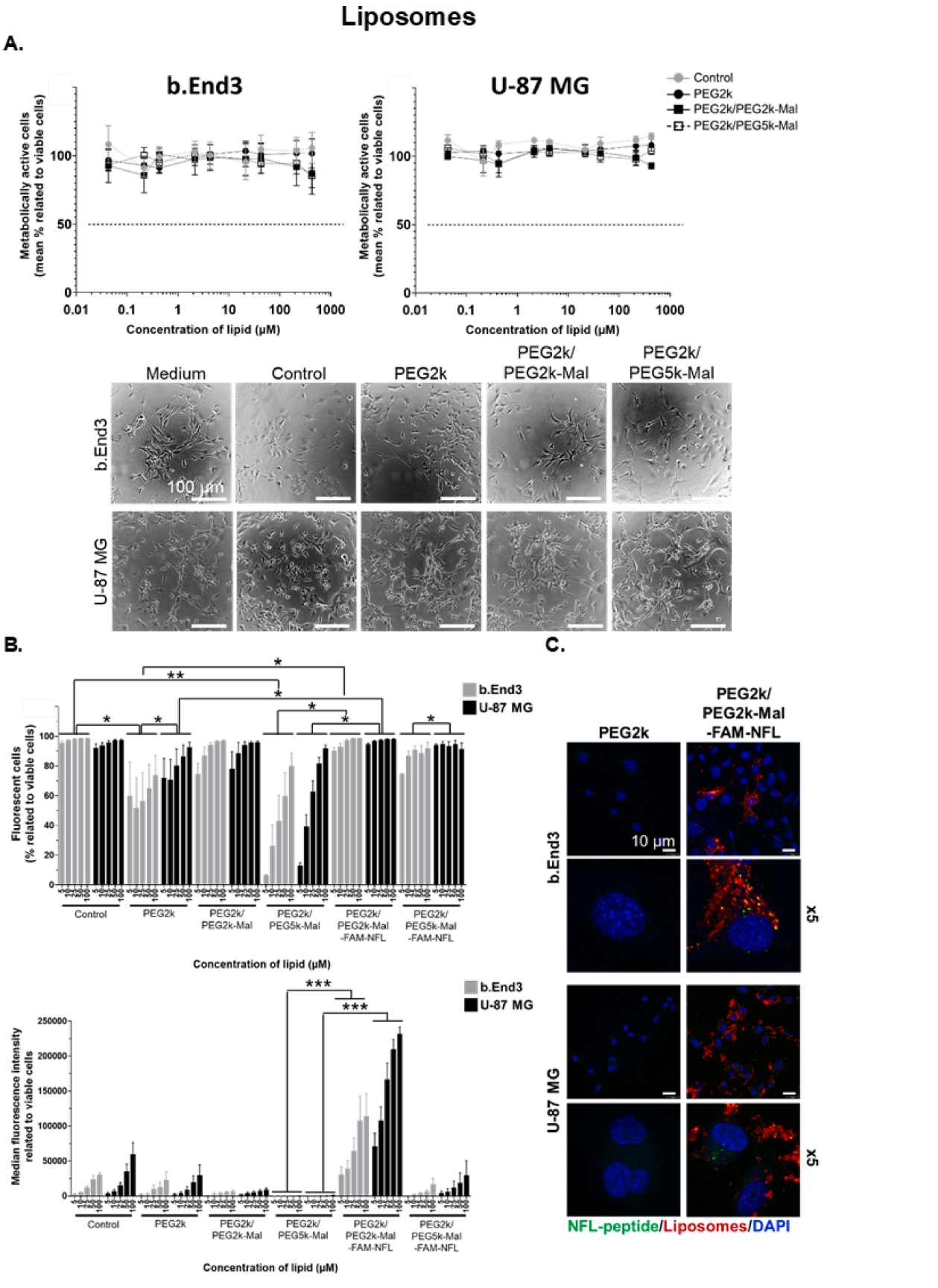

(caption on next page)

Fig. 4. *In vitro* effects of the liposome formulations on cell viability and internalization in murine b.End3 endothelial cells and human U-87 MG GBM cells. A) Murine endothelial cells (b.End3) and human GBM cells (U-87 MG) were treated for 72 h at 37 °C with increasing concentrations of liposomes (from 0.043 μM to 430 μM) and cell viability (metabolically active cells) was evaluated by MTS assay. Experiments were performed at least 3 times (n = 3). Data are represented as mean ± SEM. Images taken with an optical microscope to illustrate the morphology of cells treated with these peptides. Scale bars: 100 μm. B) A flow cytometry analysis of murine endothelial cells (b.End3, grey) and human GBM cells (U-87 MG, black) treated with increasing concentrations of liposomes (5; 10; 25; 50 and 100 μM) for 6 h at 37 °C. Results were expressed in percentage of fluorescent cells (upper) and in median fluorescence intensity (bottom) related to viable cells. Experiments were performed at least 3 times (n = 3–5), and 10,000 cells were measured for each experiment. Data are represented as mean ± SEM. Statistical analysis: Kruskall-Wallis test and followed by a Dunn's post-hoc test (*$p < 0.05$; **$p < 0.01$ and ***$p < 0.001$). C) b.End3 and U-87 MG cells were incubated 6 h at 37 °C without (Medium) or with 100 μM of PEG2k and PEG2k/PEG2K-Mal-FAM-NFL liposomes, and fluorescent labelling was realized to reveal liposomes (DiD, red), peptide (FAM-NFL peptide, green) and nuclei (DAPI, blue). Experiments were performed at least 3 times (n = 3), and images were taken with a confocal microscope. Scale bars: 10 μm. (For interpretation of the references to colour in this figure legend, the reader is referred to the web version of this article.)

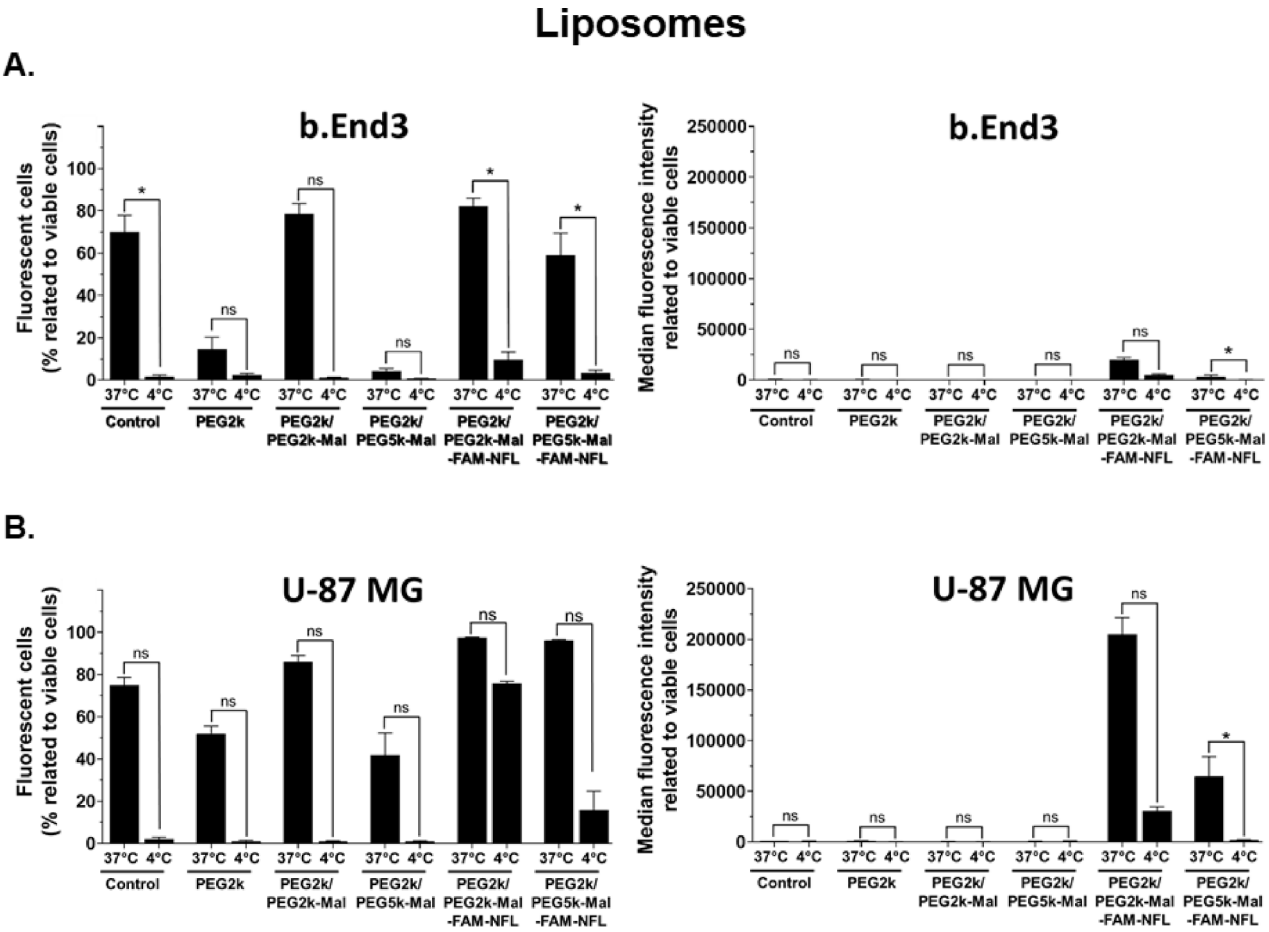

Fig. 5. Temperature effect on the internalization of liposomal formulations in murine b.End3 endothelial and human U-87 MG GBM cells**.** (A-B) A flow cytometry analysis of b.End3 (A) and U-87 MG cells (B) pre-incubated at 37 °C or at 4 °C for 1 h and treated with 100 μM liposomes for 1 h at 37 °C and 4 °C. Results were expressed in percentage of fluorescent cells (left) and in median fluorescence intensity (right) related to viable cells. Experiments were performed at least 4 times (n = 4), and 10,000 cells were measured for each experiment. Data are represented as mean ± SEM. Statistical analysis: Mann-Whitney test (ns $p > 0.05$ and *$p < 0.05$).

colleagues showed that after 5 days, TEER measurement across the b. End3 monolayer was 28.1 ± 2.3 Ω.cm^2 (Sun et al., 2022).

In a pathophysiological context such as tumors, the permeability of cerebral microvessels can be altered (Arvanitis et al., 2020). The impact of the microenvironment of GBM cells (U-87 MG) on the integrity of the endothelial cell barrier (b.End3) were analyzed based on TEER values, TJ protein expression (ZO-1) and passage of standard molecules (FITC-Dextrans) through *in vitro* BBB and BBTB models. When GBM cells are cocultured with endothelial cells, the TEER value decreases significantly (Díaz-Coránguez et al., 2013; Omidi et al., 2003; Sun et al., 2022), the expression of TJ protein on endothelial cells is altered (Arvanitis et al., 2020) and FITC-Dextrans pass more through the BBTB model than BBB model (Mendes et al., 2015). All these results suggest that the micro-environment of the U-87 MG cells has an impact on increasing the permeability of the b.End3 cells and validate our *in vitro* BBB and BBTB models. NFL peptides crosses more the BBTB model than the BBB model, confirming the increased permeability of the BBB in a pathological context. However, the passage decreases when the peptide is bound to DSPE-PEG-maleimide chains. In addition, there are more FAM-NFL-GGGC-Mal-PEG2k peptides that pass through the endothelial barrier models *in vitro* than FAM-NFL-GGGC-Mal-PEG5k peptides. This can be explained by the fact that endothelial barriers limit the passage of molecules with higher molecular weight and size (Mayhan and Heistad, 1985). For example, Poller and colleagues showed that the highest permeability coefficient measured in their work was with inulin, the largest compound they tested (Poller et al., 2008). Moreover, Smith and colleagues showed that in different BBB models, the permeability co-efficients of the lowest molecular weight (sucrose) were always lower than the highest one (propanolol) (Smith et al., 2007). According to the literature and as FAM-NFL-GGGC-Mal-PEG5k displays a higher

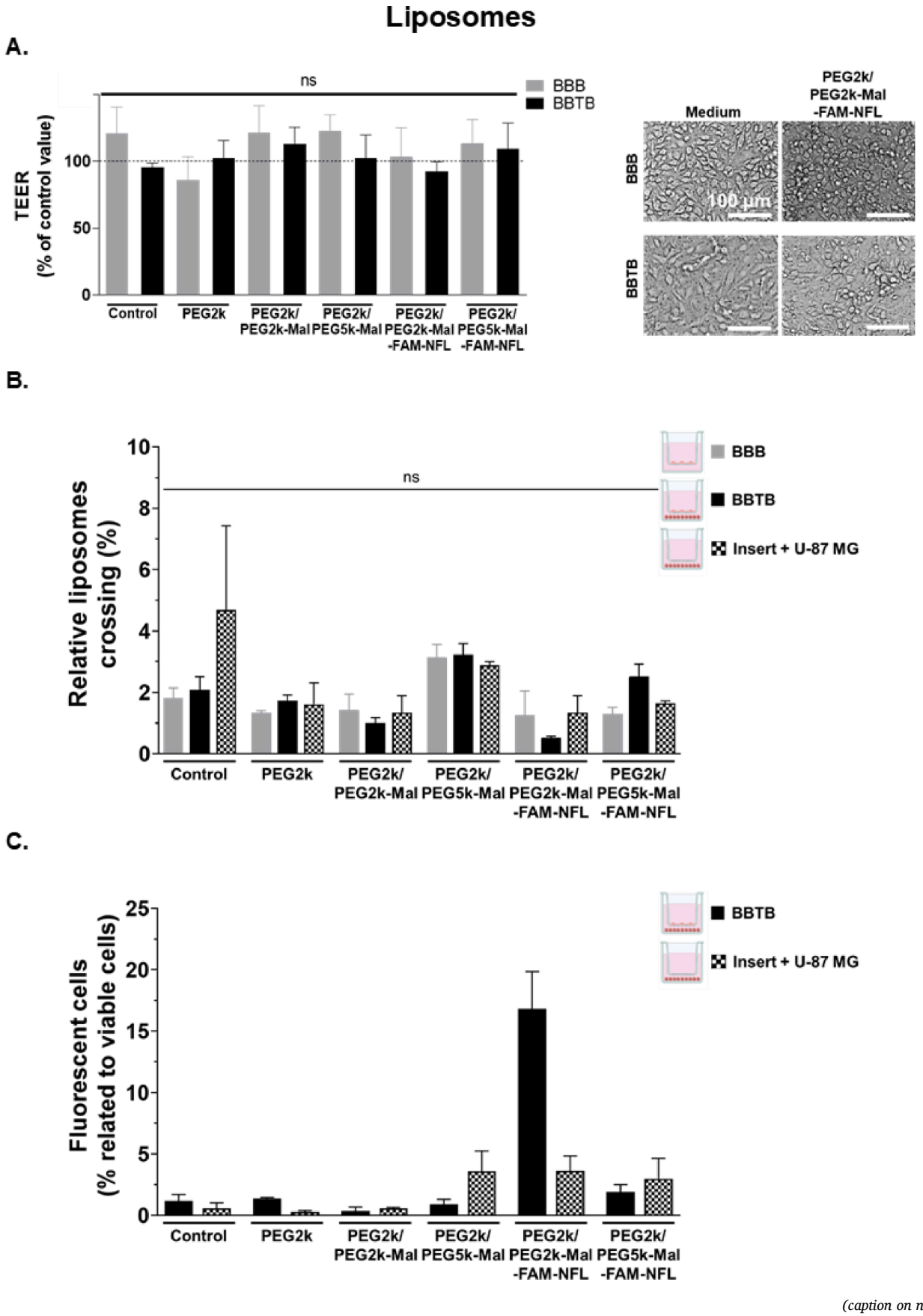

(caption on next page)

Fig. 6. Evaluation of liposomal formulations on *in vitro* BBB and BBTB models. A) The permeability of endothelial barrier of *in vitro* BBB (grey) and BBTB (black) models was assessed by measurement of the TEER values (Ohm × cm2, % of control value) after 24 h of treatment with different liposome formulations at 37 °C. Experiments were performed at least 3 times (n = 3). Data are represented as mean ± SEM. Statistical analysis by performing a Kruskall-Wallis test and a Dunn's post-hoc test (ns $p > 0.05$). Images taken with an optical microscope to illustrate the confluence of endothelial barrier cells after 24 h of treatment. Scale bars: 100 μm. B) 100 μM of liposomes were added in the luminal compartment of *in vitro* BBB (grey), BBTB (black) and insert + U-87 MG (square black and white) models for 24 h at 37 °C. The permeability of each model was assessed by calculating the quantity of liposomes in abluminal compartment compared to the initial quantity in luminal compartment and was expressed as relative crossing material percentage (at the equilibrium between each compartment). Experiments were performed at least 3 times (n = 3–7). Data are represented as mean ± SEM. Statistical analysis: Kruskall-Wallis test and a Dunn's post-hoc test (ns $p > 0.05$). C) A flow cytometry analysis of human GBM cells (U-87 MG) was realized after passage of the liposomal formulations through the endothelial monolayer cells for 24 h at 37 °C. Results were expressed in percentage of fluorescent cells related to viable cells. Experiments were performed at least 3 times (n = 3), and 10,000 cells were measured for each experiment. Data are represented as mean ± SEM. Statistical analysis: Kruskall-Wallis test and a Dunn's post-hoc test (ns $p > 0.05$, *$p < 0.05$).

molecular weight than FAM-NFL-GGGC-Mal-PEG2k (Table 1), we can suppose that the difference of crossing is due to this characteristic.

In addition, after passage of BBTB, we observed interactions of NFL peptides with GBM cells. This confirms the ability of the peptide to target GBM cells after crossing the endothelial barrier. Indeed, we observed that the NFL peptides are internalized both in GBM cells and in cancer endothelial cells (b.End3). Moreover, when the NFL peptide is coupled to liposomes, the targeting efficiency towards GBM cells is enhanced. These results were consistent with those observed in previous works. Indeed, Karim and colleagues showed that, after 6 h of treatment with LNCs with or without the NFL adsorbed at their surface, 81.9 % and 11.8 % of U-87 MG cells were fluorescent, respectively (Karim et al., 2018). When tested on GL261 cells (murine GBM), 57.7 ± 4.7 % of the cells incorporate LNCs coupled to the NFL peptide, versus 9.4 ± 3.7 % for cells treated with LNCs alone (Balzeau et al., 2013). Recently, Arib et *al.* showed that gold nanoparticles coupled to the NFL peptide can enter in F98 (GBM) and MIA PACA-2 (pancreas cancer) cells (Arib et al., 2022). Moreover, once coupled to magnetic porous silicon nanorods, more nanoparticles are detected in F98 cells (Chaix et al., 2022).

The ability of these delivery systems to enter cells are related to the nanovector and to the CPPs present at their surface. Here, our results suggest that the uptake of the different liposome formulations with or without the peptide is mainly energy dependent. Only the PEG2k/PEG2k-Mal-FAM-NFL formulation could be internalized both by an active and a passive transport, considering the results obtained compared to other liposome formulations. Unlike our results, Karim and colleagues observed only an energy-dependent internalization of LNCs combined to the FAM-NFL peptide in U-87 MG cells (Karim et al., 2018). They were surprised and explained these results by the higher rigidity and a lower permeability of lipid bilayer at low temperature. Moreover, depending on their composition, structure, and concentration, CPPs can enter cells by direct translocation and/or endocytosis (Gestin et al., 2017; Kardani et al., 2019), such as the NFL peptide that enters GBM cells through endocytic pathways and through passive transport in GBM cancer stem cells (Lépinoux-Chambaud and Eyer, 2013, 2019). When bound to large liposomes, CPPs mainly undergo endocytosis (Oller-Salvia et al., 2016). In literature, LNCs coupled to the NFL peptide are internalized in U-87 MG cells via clathrin-, caveolin-, and macropinocytosis-dependent endocytosis (Karim et al., 2018). The presence of different sizes of liposomes could influence endocytosis-dependent cellular uptake as well as passage of these objects across endothelial barriers (Danaei et al., 2018). Furthermore, the PEGylation of nanoparticles is known to influence their stability, their biodistribution as well as their ability to target. However, the length of the PEG chains seems to influence many mechanical properties of the nanoparticles, thus generating differences in the cellular mechanisms. In our experiments, Fig. 6 C shows that the chain length of the PEG coating restricts transfer across the endothelial layer and uptake in U-87 MG cells measured by flow cytometry. For a liposome coating with mPEG2k, about 17 % of all viable GBM cells bear the fluorescent label introduced by the FAM-NFL-GGGC-PEG2k/mPEG2k-liposomes. In contrast, for liposomes equally conjugated with the FAM-NFL-GGGC-peptide, but with a coating of mPEG5k, the fluorescent signal in the GBM cells is not significantly different from the controls. This result underlines the significance of the chain lengths of PEG coatings which can influence passage through the endothelial monolayer. Many studies have shown in in vitro BBB models that the PEGylation of nanocarrier with PEG chains of different sizes influenced the rate of endocytosis and transcytosis of nanocarriers, but also could lead to cytotoxicity and a different inflammatory response. The work of Tehrani and colleagues showed that the chain length of PEG could modify the surface mechanical properties of nanoparticles, which could have an impact on their interactions with cells and therefore influence the preferential pathway of cell entry (Tehrani et al., 2019). Additionally, Xie and colleagues tested liposomes modified with PEGs of different sizes (PEG400, PEG1000, PEG2000) and they demonstrated better cerebral delivery efficiency for liposomes with PEG1000 (Xie et al., 2012). Liu and colleagues developed liposomes functionalized with the cell-penetrating peptide R8-dGR, which could bind to both integrin αvβ3 and neuropilin-I receptors (Liu et al., 2016). The R8-dGR-conjugated liposomes could cross the b.End3 monolayer *in vitro*, showing the ability of this nanocarrier to cross the BBB. Moreover, Sonali and colleagues used liposomes combined with transferrin, a ligand involved in receptor-mediated transcytosis, to improve the BBB passage of docetaxel in rat brain (Sonali et al., 2016). The hydrodynamic diameter and PdI of their liposomes are similar to those we obtained with liposomes combined to the NFL peptides, suggesting that this type of transcytosis could be used by our liposomes. More detailed studies of endothelial barrier passage mechanisms should therefore be carried out in order to better understand the cellular mechanisms involved in the passage of the BBB and thus optimize the nanocarriers. Moreover, further investigations could be realized to determine the pathways involved in the transport of the liposome formulations in this study in endothelial and GBM cells using of endocytosis inhibitors, or by inhibiting efflux pumps (Arvanitis et al., 2020).

In the case of PEGylated liposomes functionalized with the FAM-NFL peptide, we can observe an *in vitro* passage through the endothelial cell barriers of < 5 %, without significant difference between BBB and BBTB. But interestingly, one of the liposome formulations, the PEG2k/PEG2k-Mal-FAM-NFL, showed a significantly higher internalization in GBM cells after passage through the endothelial barrier, compared to the other formulations. We can suppose that the low crossing of this formulation is due to their internalization in the GBM cells as we observed a high internalization in U-87 MG in monoculture (Fig. 4B). As they are internalized, they could not be detected in the abluminal compartment which can explain the low passage. This formulation,

Table 1
Description of various NFL-peptides.

Name sample	Peptide sequence	Molecular weight
FAM-NFL	5′6FAM-YSSYSAPVSSSLSVRRSYSSSSGS	2846
FAM-NFL-GGGC	5′FAM-YSSYSAPVSSSLSVRRSYSSSSGSGGGC	3120
FAM-NFL-GGGC-Mal-PEG2k	5′FAM-YSSYSAPVSSSLSVRRSYSSSSGSGGGC-Mal-PEG2k	5290
FAM-NFL-GGGC-Mal-PEG5k	5′FAM-YSSYSAPVSSSLSVRRSYSSSSGSGGGC-Mal- PEG5k	8290

combining PEG2k/PEG2k-Mal liposome with the FAM-NFL-GGGC peptide, appears to be the most efficient and promising delivery system to cross the BBB and target GBM cells. These results showed that DSPE-PEG2k-Mal is less restrictive of liposome passage across the endothelial barrier than DSPE-PEG5k-Mal.

Furthermore, it would be interesting to confirm these results after intravenous administration of this liposome formulation in GBM-bearing mice during further studies to evaluate its biodistribution and the targeting of GBM tissue after BBB passage. Most of previous works performed on similar *in vitro* BBB and BBTB models studied here, showed that the passage of liposomes functionalized with various CPPs is between 1 (Lv et al., 2013) and 15 % (Xin et al., 2021). These values seem low but show an improvement of the passage of the liposomes thanks to the modification of their surface. In addition, when these liposomes are injected intravenously into GBM-bearing mice, the functionalized liposomes are mainly found in the brain compared to liposomes without surface modification (Dos Santos Rodrigues et al., 2020b, 2020a; Lv et al., 2013; Torstensson et al., 2013; Xin et al., 2021). The optimization of BBB passage *in vivo* by such a delivery system combining a CPP with liposomes was notably described recently by Xin et al. They developed liposomes encapsulating paclitaxel (PTX) and modified on their surface with the peptide derived from the rabies virus glycoprotein (RVG), that binds to nicotinic acetylcholine receptors, widely overexpressed on BBB and glioma cells. Compared to free PTX or free liposomes, PTX-RVG liposomes have been shown to promote passage through the BBB and improve drug biodistribution and brain PTX accumulation *in vivo* (Xin et al., 2021). Lainé and colleagues showed that, when the LNC-NFL were injected in the carotid of rat bearing orthotopic GBM, an increase in survival was observed for almost half of the animals (5/12) up to 44 days, whereas the rats treated with LNCs without NFL peptide did not survive after 26 days (Lainé et al., 2012). Balzeau et al. showed that LNC have targeted to the tumor when they are functionalized with the NFL-TBS.40–63 peptide, while many LNC are not localized to the tumor when they are not functionalized with the peptide. In fact, while almost all the fluorescence is localized to the tumor when the animals are treated with the LNC functionalized with the NFL-TBS.40–63 peptide, several fluorescent signals can be found in the left hemisphere (which does not contain the tumor) when the LNC are not functionalized with the peptide (Balzeau et al., 2013). These results suggest a better crossing of the BBB when nanoparticles are combined with the NFL peptide. These results suggest a better crossing of the BBB when nanoparticles are combined with the NFL peptide.

5. Conclusion

In this study, we have shown that surface-functionalization with NFL peptide can enhance the uptake of liposomes in human GBM cells in a time and dose-dependent manner. Additionally, the peptide functionalized liposomes were preferentially internalized into GBM cells compared to cancer endothelial cells showing the targeting capacity of the nanocarrier. These results showed a higher targeting of GBM than endothelial cells by the NFL-TBS.40–63 peptide and its ability to cross the endothelial barrier. Coupled to liposomes, the peptide enhances their internalization in GBM cells compared to liposomes without the peptide. These data indicates that the NFL-TBS.40–63 peptide offers a promising tool for the GBM targeting after passage through the endothelial barrier. Indeed, to improve liposome passage through the BBTB and targeting GBM cells, it would seem interesting to formulate dual-functionalized liposomes with the NFL peptide and other peptides, ligands of receptors of the brain endothelium, known to improve the passage of the BBB. Also, it would be interesting to evaluate the biodistribution and the targeting of GBM tissue of the new formulation after BBB passage in GBM-bearing mice.

Funding Source

The European project RELIEF, selected by the intergovernmental association for the promotion of innovation EUREKA! within the framework of its twelfth call for projects Eurostars [Project ID: E! 113670]. It was co-funded by European Union's research and innovation programme Horizon 2020 with the support of Bpifrance Financement.

CRediT authorship contribution statement

Adélie Mellinger: Conceptualization, Methodology, Validation, Formal analysis, Investigation, Writing – original draft, Visualization, Project administration. **Larissa J. Lubitz:** Conceptualization, Methodology, Validation, Formal analysis, Writing – review & editing. **Claire Gazaille:** Writing – review & editing. **Gero Leneweit:** Conceptualization, Project administration. **Guillaume Bastiat:** Formal analysis, Writing – review & editing. **Claire Lépinoux-Chambaud:** Conceptualization, Validation, Project administration, Supervision, Funding acquisition. **Joël Eyer:** Conceptualization, Supervision.

Declaration of Competing Interest

Joël Eyer is one of the inventors of the NFL-TBS.40-63 peptide used in the article (WO2005121172 and WO2011073207A1) and to which GlioCure SA holds exclusive worldwide rights. Joël Eyer and Claire Lépinoux-Chambaud are cofounders of GlioCure SA and hold shares of the company. In addition, Adélie Mellinger, Claire Gazaille and Claire Lépinoux-Chambaud are employees of GlioCure SA..

Data availability

Data will be made available on request.

Acknowledgments

The authors acknowledge Rodolphe Perrot from SCIAM (Service Commun d'Imageries et d'Analyses Microscopiques), and Catherine Guillet from PACeM (Plateforme d'Analyses Cellulaire et Moléculaire).

Appendix A. Supplementary data

Supplementary data to this article can be found online at https://doi.org/10.1016/j.ijpharm.2023.123421.

References

Abbott, N.J., 2002. Astrocyte-endothelial interactions and blood-brain barrier permeability. J. Anat. 200, 629–638. https://doi.org/10.1046/j.1469-7580.2002.00064.x.

Abbott, N.J., Patabendige, A.A.K., Dolman, D.E.M., Yusof, S.R., Begley, D.J., 2010. Structure and function of the blood-brain barrier. Neurobiol. Dis. 37, 13–25. https://doi.org/10.1016/j.nbd.2009.07.030.

Alexander, A., Agrawal, M., Uddin, A., Siddique, S., Shehata, A.M., Shaker, M.A., Ata Ur Rahman, S., Abdul, M.I.M., Shaker, M.A., 2019. Recent expansions of novel strategies towards the drug targeting into the brain. Int J Nanomedicine. 14, 5895–5909. https://doi.org/10.2147/IJN.S210876.

Alnemeh-Al Ali, H., Griveau, A., Artzner, F., Dupont, A., Lautram, N., Jourdain, M.A., Eyer, J., 2022. Investigation on the self-assembly of the NFL-TBS.40-63 peptide and its interaction with gold nanoparticles as a delivery agent for glioblastoma. Int J Pharm X 4, 100128. https://doi.org/10.1016/j.ijpx.2022.100128.

Altai, M., Honarvar, H., Wållberg, H., Strand, J., Varasteh, Z., Rosestedt, M., Orlova, A., Dunås, F., Sandström, M., Löfblom, J., Tolmachev, V., Ståhl, S., 2014. Selection of an optimal cysteine-containing peptide-based chelator for labeling of affibody molecules with (188)Re. Eur. J. Med. Chem. 87, 519–528. https://doi.org/10.1016/j.ejmech.2014.09.082.

Arib, C., Griveau, A., Eyer, J., Spadavecchia, J., 2022. Cell penetrating peptide (CPP) gold(iii) - complex - bioconjugates: from chemical design to interaction with cancer cells for nanomedicine applications. Nanoscale Adv. 4, 3010–3022. https://doi.org/10.1039/d2na00096b.

Arvanitis, C.D., Ferraro, G.B., Jain, R.K., 2020. The blood–brain barrier and blood–tumour barrier in brain tumours and metastases. Nat. Rev. Cancer 20, 26–41. https://doi.org/10.1038/s41568-019-0205-x.

Balzeau, J., Pinier, M., Berges, R., Saulnier, P., Benoit, J.-P., Eyer, J., 2013. The effect of functionalizing lipid nanocapsules with NFL-TBS.40-63 peptide on their uptake by glioblastoma cells. Biomaterials 3381–3389. https://doi.org/10.1016/j.biomaterials.2013.01.068.

Berges, R., Balzeau, J., Peterson, A.C., Eyer, J., 2012a. A Tubulin Binding Peptide Targets Glioma Cells Disrupting Their Microtubules, Blocking Migration, and Inducing Apoptosis. Mol. Ther. 1367–1377 https://doi.org/10.1038/mt.2012.45.

Berges, R., Balzeau, J., Takahashi, M., Prevost, C., Eyer, J., 2012b. Structure-Function Analysis of the Glioma Targeting NFL-TBS.40-63 Peptide Corresponding to the Tubulin-Binding Site on the Light Neurofilament Subunit. PLoS One e49436. https://doi.org/10.1371/journal.pone.0049436.

Blakeley, J., 2008. Drug delivery to brain tumors. Curr. Neurol. Neurosci. Rep. 8, 235–241. https://doi.org/10.1007/s11910-008-0036-8.

Booth, R., Kim, H., 2012. Characterization of a microfluidic in vitro model of the blood-brain barrier (μBBB). Lab Chip 12, 1784–1792. https://doi.org/10.1039/c2lc40094d.

Briuglia, M.-L., Rotella, C., McFarlane, A., Lamprou, D.A., 2015. Influence of cholesterol on liposome stability and on in vitro drug release. Drug Deliv. Transl. Res. 5, 231–242. https://doi.org/10.1007/s13346-015-0220-8.

Bruinsmann, F.A., Richter Vaz, G., de Cristo Soares Alves, A., Aguirre, T., Raffin Pohlmann, A., Stanisçuaski Guterres, S., Sonvico, F., 2019. Nasal Drug Delivery of Anticancer Drugs for the Treatment of Glioblastoma: Preclinical and Clinical Trials. Molecules 24, 4312. https://doi.org/10.3390/molecules24234312.

Carradori, D., Saulnier, P., Préat, V., des Rieux, A., Eyer, J., 2016. NFL-lipid nanocapsules for brain neural stem cell targeting in vitro and in vivo. J Control Release 238, 253–262. https://doi.org/10.1016/j.jconrel.2016.08.006.

Chaix, A., Griveau, A., Defforge, T., Grimal, V., Le Borgne, B., Gautier, G., Eyer, J., 2022. Cell penetrating peptide decorated magnetic porous silicon nanorods for glioblastoma therapy and imaging. RSC Adv. 12, 11708–11714. https://doi.org/10.1039/d2ra00508e.

Chung, K., Ullah, I., Kim, N., Lim, J., Shin, J., Lee, S.C., Jeon, S., Kim, S.H., Kumar, P., Lee, S.-K., 2020. Intranasal delivery of cancer-targeting doxorubicin-loaded PLGA nanoparticles arrests glioblastoma growth. J. Drug Target. 28, 617–626. https://doi.org/10.1080/1061186X.2019.1706095.

Constantinescu, C.A., Fuior, E.V., Rebleanu, D., Deleanu, M., Simion, V., Voicu, G., Escriou, V., Manduteanu, I., Simionescu, M., Calin, M., 2019. Targeted Transfection Using PEGylated Cationic Liposomes Directed Towards P-Selectin Increases siRNA Delivery into Activated Endothelial Cells. Pharmaceutics. 11, 47. https://doi.org/10.3390/pharmaceutics11010047.

Corrêa, A.C.N.T.F., Vericimo, M.A., Dashevskiy, A., Pereira, P.R., Paschoalin, V.M.F., 2019. Liposomal Taro Lectin Nanocapsules Control Human Glioblastoma and Mammary Adenocarcinoma Cell Proliferation. Molecules 24, 471. https://doi.org/10.3390/molecules24030471.

Dai, T., Jiang, K., Lu, W., 2018. Liposomes and lipid disks traverse the BBB and BBTB as intact forms as revealed by two-step Förster resonance energy transfer imaging. Acta Pharm. Sin. B 8, 261–271. https://doi.org/10.1016/j.apsb.2018.01.004.

Danaei, M., Dehghankhold, M., Ataei, S., Hasanzadeh Davarani, F., Javanmard, R., Dokhani, A., Khorasani, S., Mozafari, M.R., 2018. Impact of Particle Size and Polydispersity Index on the Clinical Applications of Lipidic Nanocarrier Systems. Pharmaceutics 10, 57. https://doi.org/10.3390/pharmaceutics10020057.

Díaz-Coránguez, M., Segovia, J., López-Ornelas, A., Puerta-Guardo, H., Ludert, J., Chávez, B., Meraz-Cruz, N., González-Mariscal, L., 2013. Transmigration of neural stem cells across the blood brain barrier induced by glioma cells. PLoS One 8, e60655.

Dos Santos Rodrigues, B., Arora, S., Kanekiyo, T., Singh, J., 2020a. Efficient neuronal targeting and transfection using RVG and transferrin-conjugated liposomes. Brain Res. 1734, 146738 https://doi.org/10.1016/j.brainres.2020.146738.

Dos Santos Rodrigues, B., Lakkadwala, S., Kanekiyo, T., Singh, J., 2020b. Dual-Modified Liposome for Targeted and Enhanced Gene Delivery into Mice Brain. J. Pharmacol. Exp. Ther. 374, 354–365. https://doi.org/10.1124/jpet.119.264127.

Downs, M.E., Buch, A., Sierra, C., Karakatsani, M.E., Teichert, T., Chen, S., Konofagou, E. E., Ferrera, V.P., 2015. Long-Term Safety of Repeated Blood-Brain Barrier Opening via Focused Ultrasound with Microbubbles in Non-Human Primates Performing a Cognitive Task. PLoS One 10, e0125911.

Gestin, M., Dowaidar, M., Langel, Ü., 2017. Uptake Mechanism of Cell-Penetrating Peptides. Adv. Exp. Med. Biol. 1030, 255–264. https://doi.org/10.1007/978-3-319-66095-0_11.

Gloor, S.M., Wachtel, M., Bolliger, M.F., Ishihara, H., Landmann, R., Frei, K., 2001. Molecular and cellular permeability control at the blood-brain barrier. Brain Res. Brain Res. Rev. 36, 258–264. https://doi.org/10.1016/s0165-0173(01)00102-3.

Grech, N., Dalli, T., Mizzi, S., Meilak, L., Calleja, N., Zrinzo, A., 2020. Rising Incidence of Glioblastoma Multiforme in a Well-Defined Population. Cureus. 12, e8195.

Griveau, A., Alnemeh-Al Ali, H., Jourdain, M.A., Dupont, A., Eyer, J., 2022. Characterization and quantification of the interaction between the NFL-TBS.40-63 peptide and lipid nanocapsules. Int J Pharm X 4, 100127. https://doi.org/10.1016/j.ijpx.2022.100127.

Groothuis, D.R., 2000. The blood-brain and blood-tumor barriers: a review of strategies for increasing drug delivery. Neuro Oncol. 2, 45–59. https://doi.org/10.1093/neuonc/2.1.45.

Jhaveri, A., Deshpande, P., Pattni, B., Torchilin, V., 2018. Transferrin-targeted, resveratrol-loaded liposomes for the treatment of glioblastoma. J. Control. Release 277, 89–101. https://doi.org/10.1016/j.jconrel.2018.03.006.

Johnson, D.R., O'Neill, B.P., 2012. Glioblastoma survival in the United States before and during the temozolomide era. J. Neurooncol 107, 359–364. https://doi.org/10.1007/s11060-011-0749-4.

Juhairiyah, F., de Lange, E.C.M., 2021. Understanding Drug Delivery to the Brain Using Liposome-Based Strategies: Studies that Provide Mechanistic Insights Are Essential. AAPS J. 23, 114. https://doi.org/10.1208/s12248-021-00648-z.

Kardani, K., Milani, A., H Shabani, S., Bolhassani, A., 2019. Cell penetrating peptides: the potent multi-cargo intracellular carriers. Expert Opin Drug Deliv. 16, 1227–1258. https://doi.org/10.1080/17425247.2019.1676720.

Karim, R., Lepeltier, E., Esnault, L., Pigeon, P., Lemaire, L., Lépinoux-Chambaud, C., Clere, N., Jaouen, G., Eyer, J., Piel, G., Passirani, C., 2018. Enhanced and preferential internalization of lipid nanocapsules into human glioblastoma cells: effect of a surface-functionalizing NFL peptide. Nanoscale 10, 13485–13501. https://doi.org/10.1039/c8nr02132e.

Katona, G., Sabir, F., Sipos, B., Naveed, M., Schelz, Z., Zupkó, I., Csóka, I., 2022. Development of Lomustine and n-Propyl Gallate Co-Encapsulated Liposomes for Targeting Glioblastoma Multiforme via Intranasal Administration. Pharmaceutics. 14, 631. https://doi.org/10.3390/pharmaceutics14030631.

Khan, A.R., Yang, X., Fu, M., Zhai, G., 2018. Recent progress of drug nanoformulations targeting to brain. J. Control. Release 291, 37–64. https://doi.org/10.1016/j.jconrel.2018.10.004.

Lainé, A.-L., Huynh, N.T., Clavreul, A., Balzeau, J., Béjaud, J., Vessieres, A., Benoit, J.-P., Eyer, J., Passirani, C., 2012. Brain tumour targeting strategies via coated ferrociphenol lipid nanocapsules. European Journal of Pharmaceutics and Biopharmaceutics. Eur. J. Pharm. Biopharm. 690–693. https://doi.org/10.1016/j.ejpb.2012.04.012.

Lépinoux-Chambaud, C., Eyer, J., 2013. The NFL-TBS.40-63 anti-glioblastoma peptide enters selectively in glioma cells by endocytosis. Int. J. Pharm. 454, 738–747. https://doi.org/10.1016/j.ijpharm.2013.04.004.

Lépinoux-Chambaud, C., Eyer, J., 2019. The NFL-TBS.40-63 peptide targets and kills glioblastoma stem cells derived from human patients and also targets nanocapsules into these cells. Int. J. Pharm. 566, 218–228. https://doi.org/10.1016/j.ijpharm.2019.05.060.

Lipinski, C.A., Lombardo, F., Dominy, B.W., Feeney, P.J., 2001. Experimental and computational approaches to estimate solubility and permeability in drug discovery and development settings. Adv. Drug Deliv. Rev. 46, 3–26. https://doi.org/10.1016/s0169-409x(00)00129-0.

Liu, Y., Mei, L., Xu, C., Yu, Q., Shi, K., Zhang, L., Wang, Y., Zhang, Q., Gao, H., Zhang, Z., He, Q., 2016. Dual Receptor Recognizing Cell Penetrating Peptide for Selective Targeting, Efficient Intratumoral Diffusion and Synthesized Anti-Glioma Therapy. Theranostics 6, 177–191. https://doi.org/10.7150/thno.13532.

Louis, D.N., Ohgaki, H., Wiestler, O.D., Cavenee, W.K., Burger, P.C., Jouvet, A., Scheithauer, B.W., Kleihues, P., 2007. The 2007 WHO classification of tumours of the central nervous system. Acta Neuropathol. 114, 97–109. https://doi.org/10.1007/s00401-007-0243-4.

Lv, Q., Li, L.-M., Han, M., Tang, X.-J., Yao, J.-N., Ying, X.-Y., Li, F.-Z., Gao, J.-Q., 2013. Characteristics of sequential targeting of brain glioma for transferrin-modified cisplatin liposome. Int. J. Pharm. 444, 1–9. https://doi.org/10.1016/j.ijpharm.2013.01.025.

Mayhan, W.G., Heistad, D.D., 1985. Permeability of blood-brain barrier to various sized molecules. Am. J. Phys. Anthropol. 248, H712–H718. https://doi.org/10.1152/ajpheart.1985.248.5.H712.

Mendes, B., Marques, C., Carvalho, I., Costa, P., Martins, S., Ferreira, D., Sarmento, B., 2015. Influence of glioma cells on a new co-culture in vitro blood-brain barrier model for characterization and validation of permeability. Int. J. Pharm. 490, 94–101. https://doi.org/10.1016/j.ijpharm.2015.05.027.

Mozar, F.S., Chowdhury, E.H., 2018. Impact of PEGylated Nanoparticles on Tumor Targeted Drug Delivery. Curr. Pharm. Des. 24, 3283–3296. https://doi.org/10.2174/1381612824666180730161721.

Nakagawa, S., Deli, M.A., Kawaguchi, H., Shimizudani, T., Shimono, T., Kittel, Á., Tanaka, K., Niwa, M., 2009. A new blood–brain barrier model using primary rat brain endothelial cells, pericytes and astrocytes. Neurochem. Int. 54 (3–4), 253–263. https://doi.org/10.1016/j.neuint.2008.12.002.

Obermeier, B., Daneman, R., Ransohoff, R.M., 2013. Development, maintenance and disruption of the blood-brain barrier. Nat. Med. 19, 1584–1596. https://doi.org/10.1038/nm.3407.

Oike, T., Suzuki, Y., Sugawara, K., Shirai, K., Noda, S., Tamaki, T., Nagaishi, M., Yokoo, H., Nakazato, Y., Nakano, T., 2013. Radiotherapy plus concomitant adjuvant temozolomide for glioblastoma: Japanese mono-institutional results. PLoS One 8, e78943.

Oller-Salvia, B., Sánchez-Navarro, M., Giralt, E., Teixidó, M., 2016. Blood-brain barrier shuttle peptides: an emerging paradigm for brain delivery. Chem. Soc. Rev. 45, 4690–4707. https://doi.org/10.1039/c6cs00076b.

Omidi, Y., Campbell, L., Barar, J., Connell, D., Akhtar, S., Gumbleton, M., 2003. Evaluation of the immortalised mouse brain capillary endothelial cell line, b.End3, as an in vitro blood-brain barrier model for drug uptake and transport studies. Brain Res. 990, 95–112. https://doi.org/10.1016/s0006-8993(03)03443-7.

Ostrom, Q.T., Gittleman, H., Liao, P., Vecchione-Koval, T., Wolinsky, Y., Kruchko, C., Barnholtz-Sloan, J.S., 2017. CBTRUS Statistical Report: Primary brain and other central nervous system tumors diagnosed in the United States in 2010–2014. Neuro Oncol. 19, v1–v88. https://doi.org/10.1093/neuonc/nox158.

Ostrom, Q.T., Price, M., Neff, C., Cioffi, G., Waite, K.A., Kruchko, C., Barnholtz-Sloan, J. S., 2022. CBTRUS Statistical Report: Primary Brain and Other Central Nervous System Tumors Diagnosed in the United States in 2015–2019. Neuro Oncol. 24, v1–v95. https://doi.org/10.1093/neuonc/noac202.

Pardridge, W.M., 2002. Drug and gene delivery to the brain: the vascular route. Neuron 36, 555–558. https://doi.org/10.1016/s0896-6273(02)01054-1.

Park, J.S., Choe, K., Khan, A., Jo, M.H., Park, H.Y., Kang, M.H., Park, T.J., Kim, M.O., 2023. Establishing Co-Culture Blood-Brain Barrier Models for Different

Neurodegeneration Conditions to Understand Its Effect on BBB Integrity. Int. J. Mol. Sci. 24, 5283. https://doi.org/10.3390/ijms24065283.
Poller, B., Gutmann, H., Krähenbühl, S., Weksler, B., Romero, I., Couraud, P.-O., Tuffin, G., Drewe, J., Huwyler, J., 2008. The human brain endothelial cell line hCMEC/D3 as a human blood-brain barrier model for drug transport studies. J. Neurochem. 107 (5), 1358–1368. https://doi.org/10.1111/j.1471-4159.2008.05730.x.
Saka, R., Sathe, P., Khan, W., 2019. 11 - Brain local delivery strategy. In: Gao, H., Gao, X. (Eds.), Brain Targeted Drug Delivery System. Academic Press, pp. 241–286. https://doi.org/10.1016/B978-0-12-814001-7.00011-1.
Sheikov, N., McDannold, N., Sharma, S., Hynynen, K., 2008. Effect of focused ultrasound applied with an ultrasound contrast agent on the tight junctional integrity of the brain microvascular endothelium. Ultrasound Med. Biol. 34, 1093–1104. https://doi.org/10.1016/j.ultrasmedbio.2007.12.015.
Smith, M., Omidi, Y., Gumbleton, M., 2007. Primary porcine brain microvascular endothelial cells: Biochemical and functional characterisation as a model for drug transport and targeting. J. Drug Target. 15, 253–268. https://doi.org/10.1080/10611860701288539.
Sonali, Singh, R. P., Singh, N., Sharma, G., Vijayakumar, M. R., Koch, B., Singh, S., Singh, U., Dash, D., Pandey, B. L., & Muthu, M. S., 2016. Transferrin liposomes of docetaxel for brain-targeted cancer applications: formulation and brain theranostics. Drug deliv., 23(4), 1261–1271. https://doi.org/10.3109/10717544.2016.1162878.
Sun, J., Ou, W., Han, D., Paganini-Hill, A., Fisher, M.J., Sumbria, R.K., 2022. Comparative studies between the murine immortalized brain endothelial cell line (b. End3) and induced pluripotent stem cell-derived human brain endothelial cells for paracellular transport. PLoS One 17, e0268860.
Tai, J., Han, M., Lee, D., Park, I.-H., Lee, S.H., Kim, T.H., 2022. Different Methods and Formulations of Drugs and Vaccines for Nasal Administration. Pharmaceutics 14, 1073. https://doi.org/10.3390/pharmaceutics14051073.
Tehrani, S.F., Bernard-Patrzynski, F., Puscas, I., Leclair, G., Hildgen, P., Roullin, V.G., 2019. Length of surface PEG modulates nanocarrier transcytosis across brain vascular endothelial cells. Nanomedicine 16, 185–194. https://doi.org/10.1016/j.nano.2018.11.016.
Tong, H., Wang, Y., Lu, X., Wang, P., Zhao, S., Chang, H., Yu, X., 2015. On the preparation of transferrin modified artesunate nanoliposomes and their glioma-targeting treatment in-vitro and in-vivo. Int. J. Clin. Exp. Med. 8, 22045–22052.
Torstensson, G.N.J., Torp, T.L., Rasuli-Oskuii, N., Kjeldsen, B.J., 2013. Graft flow unaffected by full occlusion of left anterior descending artery during coronary artery bypass grafting in a porcine model. Heart Surg. Forum 16, E107–E113. https://doi.org/10.1532/HSF98.20121112.
Van Meir, E.G., Hadjipanayis, C.G., Norden, A.D., Shu, H.-K., Wen, P.Y., Olson, J.J., 2010. Exciting new advances in neuro-oncology: the avenue to a cure for malignant glioma. CA Cancer J. Clin. 60, 166–193. https://doi.org/10.3322/caac.20069.
Van Tellingen, O., Yetkin-Arik, B., de Gooijer, M.C., Wesseling, P., Wurdinger, T., de Vries, H.E., 2015. Overcoming the blood–brain tumor barrier for effective glioblastoma treatment. Drug Resist. Updat. 19, 1–12. https://doi.org/10.1016/j.drup.2015.02.002.
Wei, H.-J., Upadhyayula, P.S., Pouliopoulos, A.N., Englander, Z.K., Zhang, X., Jan, C.-I., Guo, J., Mela, A., Zhang, Z., Wang, T.J.C., Bruce, J.N., Canoll, P.D., Feldstein, N.A., Zacharoulis, S., Konofagou, E.E., Wu, C.-C., 2021. Focused Ultrasound-Mediated Blood-Brain Barrier Opening Increases Delivery and Efficacy of Etoposide for Glioblastoma Treatment. Int. J. Radiat. Oncol. Biol. Phys. 110, 539–550. https://doi.org/10.1016/j.ijrobp.2020.12.019.
Wu, W., Klockow, J.L., Zhang, M., Lafortune, F., Chang, E., Jin, L., Wu, Y., Daldrup-Link, H.E., 2021. Glioblastoma multiforme (GBM): An overview of current therapies and mechanisms of resistance. Pharmacol. Res. 171, 105780 https://doi.org/10.1016/j.phrs.2021.105780.
Xie, F., Yao, N., Qin, Y., Zhang, Q., Chen, H., Yuan, M., Tang, J., Li, X., Fan, W., Zhang, Q., Wu, Y., Hai, L., He, Q., 2012. Investigation of glucose-modified liposomes using polyethylene glycols with different chain lengths as the linkers for brain targeting. Int. J. Nanomedicine 7, 163–175. https://doi.org/10.2147/IJN.S23771.
Xin, X., Liu, W., Zhang, Z.-A., Han, Y., Qi, L.-L., Zhang, Y.-Y., Zhang, X.-T., Duan, H.-X., Chen, L.-Q., Jin, M.-J., Wang, Q.-M., Gao, Z.-G., Huang, W., 2021. Efficient Anti-Glioma Therapy Through the Brain-Targeted RVG15-Modified Liposomes Loading Paclitaxel-Cholesterol Complex. Int. J. Nanomedicine 16, 5755–5776. https://doi.org/10.2147/IJN.S318266.
Zylberberg, C., Gaskill, K., Pasley, S., Matosevic, S., 2017. Engineering liposomal nanoparticles for targeted gene therapy. Gene Ther. 24, 441–452. https://doi.org/10.1038/gt.2017.41.